

THE AUTOCRINE EXCITOTOXICITY OF ANTILLATOXIN, A NOVEL
LIPOPEPTIDE DERIVED FROM THE PANTROPICAL MARINE
CYANOBACTERIUM *LYNGBYA majuscula*

by

JOHN MICHAEL MOULTON

(Under the Direction of Dr. Thomas Murray)

ABSTRACT

Antillatoxin (ATX) is a lipopeptide produced by the marine cyanobacterium *Lyngbya majuscula*. ATX, a Na⁺ channel activator, produces N-methyl-D-aspartate (NMDA) receptor mediated neurotoxicity in rat cerebellar granule neurons (CGNs). To determine whether ATX produced this neurotoxicity through an indirect mechanism, the influence of ATX on glutamate release was ascertained. ATX produced a concentration-dependent increase in extracellular glutamate. This response was prevented by the Na⁺ channel antagonist tetrodotoxin (TTX). ATX caused a strong membrane depolarization with a magnitude comparable to that of 100 mM KCL. ATX also produced concentration-dependent cytotoxicity as measured by lactate dehydrogenase activity. Ca⁺² influx was measured using a fluorescent imaging plate reader (FLIPR). ATX produced concentration-dependent Ca⁺² influx. The neurotoxic mechanisms of ATX are therefore similar to those of brevetoxins, which produce neuronal injury through depolarization-induced Na⁺¹ load, glutamate release, relief of Mg⁺² block of NMDA receptors, and Ca⁺² influx.

INDEX WORDS: Neurotoxin, Excitotoxicity, Glutamate, Sodium Channel, FLIPR, Cerebellar Granule Neurons

THE AUTOCRINE EXCITOTOXICITY OF ANTILLATOXIN, A NOVEL
LIPOPEPTIDE DERIVED FROM THE ANTROPICAL MARINE
CYANOBACTERIUM *LYNGBYA majuscula*

by

JOHN MICHAEL MOULTON
B.S., The University of Georgia

A Thesis Submitted to the Graduate Faculty of The University of Georgia in Partial
Fulfillment of the Requirements for the Degree

MASTER OF SCIENCE

ATHENS, GEORGIA

2003

© 2003

John Michael Moulton

All Rights Reserved

THE AUTOCRINE EXCITOTOXICITY OF ANTILLATOXIN, A NOVEL
LIPOPEPTIDE DERIVED FROM THE ANTROPICAL MARINE
CYANOBACTERIUM *LYNGBYA majuscula*

by

JOHN MICHAEL MOULTON

Major Professor: Thomas Murray
Committee: Gaylen Edwards
Julie Coffield

Electronic Version Approved:

Maureen Grasso
Dean of the Graduate School
The University of Georgia
May 2003

TABLE OF CONTENTS

	Page
LIST OF FIGURES.....	v
CHAPTER	
1 Introduction.....	1
2 Literature Review.....	4
3 The Autocrine Excitotoxicity Of Antillatoxin, A Novel Lipopeptide Derived From The Pantropical Marine Cyanobacterium <i>Lyngbya</i> <i>majuscula</i>	24
REFERENCES	37

LIST OF FIGURES

	Page
Figure 1: ATX-Induced Cytotoxicity.....	45
Figure 2: Membrane-Potential Assay.....	46
Figure 3: Viability-Assay.....	47
Figure 4: Time-Dependent ATX-Stimulated Glutamate Efflux	48
Figure 5: Concentration-Dependent ATX-Mediated Glutamate Efflux	49
Figure 6: Correlation Between Glutamate Efflux and Cytotoxicity	50
Figure 7: ATX-Stimulated Ca ⁺² Influx	51
Figure 8: Correlation Between Ca ⁺² Influx and Cytotoxicity.....	52
Figure 9: Pharmacological Assessment of Glutamate Release.....	53

CHAPTER 1

Introduction

Marine cyanobacteria are major producers of biologically active and structurally unique natural products (Orjala, J. *et al.*, 1995; Yokokawa, F., *et al.*, 1999; Berman, *et al.*, 1999). These microalgal blooms have been implicated in human intoxication and extensive fish mortality (Nogle *et al.*, 2001). In addition to their ecological significance, microalgal products possess great potential as biochemical and pharmacological tools.

The pantropical cyanobacterium, *Lyngbya majuscula*, produces a diverse array of secondary metabolites, including, kalkitoxin, debromoaphysiatoxin, lyngbyatoxin, curacin-A and antillatoxin, with the latter being the focus of this study. Antillatoxin is among the most ichthyotoxic metabolites isolated to date. In humans, symptoms of *L. majuscula* include, respiratory irritation, eye inflammation, and severe contact dermatitis in exposed fishermen and swimmers (Abal, 2001). A recent report has shown that antillatoxin induces NMDA receptor-mediated neurotoxicity in primary cultures of rat cerebellar granule cells (Berman *et al.*, 1999). This was confirmed morphologically as ATX-exposed CGNs expressed swelling of neuronal somata, thinning of neurites, and blebbing of neurite membranes. ATX-induced neurotoxicity was concentration-dependent with an EC₅₀ of 20.1 ± 6.4 nM as monitored by lactate dehydrogenase efflux.

Further characterizing ATX's mechanism, Li *et al.* (2001) showed that ATX acts as an activator of voltage-gated Na⁺ channels. They found that TTX, a Na⁺ channel antagonist, blocked the increase in ATX-induced Na⁺ influx in CGNs. They also used

[³H]BTX, a radioligand probe that labels receptor site 2 on the voltage-gated Na⁺ channel, to provide direct evidence for ATX interaction with a site on the α subunit of the Na⁺ channel. Competitive binding assays revealed that ATX interacts with either neurotoxin site 4 or an undiscovered novel site. To determine directly whether ATX induces a gain of function in the Na⁺ channel, they used the ²²Na⁺ flux assay previously described by Catterall and collaborators (Catterall, 1975; Tamkun and Catterall, 1981). They found that ATX elicited a (TTX sensitive) concentration-dependent stimulation of ²²Na⁺ influx in CGNs (EC₅₀=98.2 ± 12.0 nM).

Our lab has recently shown that another class of marine algal toxin, brevetoxins, produce acute excitotoxicity in CGNs through an autocrine mechanism. Brevetoxins are lipid-soluble polyether neurotoxins that produce periodic harmful algal blooms in the Gulf of Mexico and west coast of Florida (Baden, 1989). Excitotoxicity is the excessive stimulation of neuronal glutamate receptors and resultant dysregulation of cellular Ca⁺² homeostasis that ultimately leads to cell death (Choi, 1988). Autocrine excitotoxicity refers specifically to instances where excitotoxicity is a secondary consequence of glutamate efflux (Leist *et al.*, 1997). Brevetoxins produce neuronal injury in CGNs through depolarization-evoked Na⁺ load, glutamate efflux, relief of the Mg⁺² block of the NMDA receptor, and subsequent Ca⁺² influx.

Domoic acid, a tricarboxylic amino acid analog of glutamate, is produced by the diatom *Pseudo-nitzschia multiseries* and produces a neurotoxic response in CGNs that is mediated primarily by NMDA receptors (Berman and Murray, 1997). Domoic acid-induced neurotoxicity was, however, demonstrated to be due to their activation on AMPA/kainate receptors. This activation results in membrane depolarization, which

stimulates the release of glutamate and also relieves the protective Mg^{+2} block in NMDA receptors.

The present study was to test the hypothesis that ATX acts as an autocrine excitotoxicant by inducing the release of glutamate in CGNs. Experiments were carried out in a physiologic medium at a temperature of 22°C. Reduced temperatures have previously been shown to increase the neurotoxic potency of glutamate in cultured cerebellar granule neurons (Berman and Murray, 1996). Moreover, primary cultured CGNs are currently used as a model for studying both acute and delayed glutamate-induced toxicity (Schramm *et al.*, 1990). This *in vitro* model provides a 90% homogeneous cell population expressing a glutamatergic phenotype (Cox *et al.*, 1990) and acquires some of the morphological, biochemical and electrophysiological characteristics of mature neurons (Jalonen *et al.*, 1990).

The present results confirm that ATX toxicity is due to the activation of voltage dependent Na^{+} channels. Moreover, we have shown that acute ATX cytotoxicity is associated with cellular swelling, while delayed effects depend on the efflux of endogenous glutamate. This was confirmed morphologically by staining the neurons with fluorescein diacetate-propidium iodide. Endogenous glutamate released into the media activates both the NMDA and AMPA/kainate receptors. As with brevetoxins and domoic acid, ATX may be viewed as capable of producing an autocrine excitotoxicity in CGNs.

CHAPTER 2

Literature Review

Cyanobacteria and Their Toxins

Cyanobacteria (blue-green algae) are amongst the oldest species known to this planet. These photosynthetic, Gram-negative, organisms are found both in marine and freshwater aquatic environments. Cyanobacteria typically grow best in warm, still, eutrophic or hypertrophic waters (Hunter 1998; Skulberg et al. 1984). With adequate minerals, nutrients, and a neutral or alkaline pH, mass developments in aqueous suspensions (blooms), surface scums and mats of cyanobacteria can be found. These blooms develop annually in the summer and autumn months. Though optimal viability is usually found in the temperate latitudes, seasonal mats can also form in polar environments but aren't as long lived compared to their temperate counterparts.

Animal-, bird-, fish and human-poisonings have been ascribed to cyanobacterial blooms and scums in the scientific and popular press for over a century (Codd et al., 1994). Recent investigations and analyses, indicated a cosmopolitan occurrence of toxic cyanobacterial blooms, with reports from at least 42 countries and all continents (Carmichael, 1982).

The main cyanobacterial genera that cause these poisonings include filamentous *Anabaena*, *Aphanizomenon*, *Nostoc*, *Nodularia*, *Oscillatoria*, and unicellular colonial non-, *Nostoc*, *Fodularia*, *Oscillatoria*, and unicellular colonial *Microcystis* and *Lynbya* (Ikawa et al, 1985). Cyanobacterial related illness in humans and animals are mediated through a range of toxins. These toxins can be categorized into three major groups:

hepatotoxins, neurotoxins and endotoxins. Although these toxins have been studied extensively, the factors affecting the production of these toxins are still poorly understood.

Hepatotoxins

This category of cyanobacterial toxins has most frequently been implicated in incidents of animal toxicity. Hepatotoxins diffuse across the ileum where they are transported to the liver via the portal circulation and taken up by hepatocytes. They have been reported to act as potent inhibitors of protein phosphatases types 1 and 2A, enzymes crucial to cell growth and tumor suppression (Matsushima et al. 1990).

Hepatotoxins are medium molecular weight cyclic peptide toxins. Two major hepatotoxins are microcystin and nodularin. Microcystin is a cyclic heptapeptide produced by different *Microcystis* and *Oscillatoria* strains. Nodularin, produced by *N. spumigena*, is a monocyclic pentapeptide with a molecular weight of 825.0. Both microcystin and nodularin share homologous C20 amino acid, 3-amino-9-methoxy-2, 6,8-trimethyl-10-phenyl-4, 6-decadienoic acid, β -amino group, multiple methyl side chains, and a diene unit.

Weakness, anorexia, pallor of the mucous membranes, vomiting, cold extremities and diarrhea characterize acute poisoning by hepatotoxins (Carmichael, 1992). Death due to intrahepatic hemorrhage and hypovolemic shock usually occurs within a few hours.

Neurotoxins

This particular class of cyanobacterial toxins acts directly on the central nervous system differing only in their mode of actions. Of the neurotoxins, anatoxin α , saxitoxin and neosaxitoxin are among the more common and most studied neurotoxins to date.

Anatoxin- α , isolated from *Anabaena* spp., is a potent nicotinic agonist, which causes a depolarizing neuromuscular blockade (Carmichael, 1992). Acute intoxication in laboratory animals causes muscle fasciculation, decreased movement, collapse, cyanosis, convulsions and death. Death is due to respiratory failure and occurs within minutes of administration.

Saxitoxin and neosaxitoxin, originally identified from dino-flagellates, cause paralytic shellfish poisoning. They bind to neurotoxin site 1 of the Na⁺ channel causing inhibition of Na⁺ transport across the axon membrane. Symptoms of acute poisoning include twitching, loss of coordination and irregular breathing which results in death.

Lipopolysaccharide endotoxin

Lipopolysaccharide (LPS) is an important constituent of the cyanobacterial cell wall. Cyanobacterial LPS lacks the phosphate group in the lipid A core (Keleti and Sykora, 1982). In animal experiments, injection of LPS results in conflicting results (Keleti *et al.*, 1979; Keleti and Sykora, 1982). This indicates that this class of toxin and its mode of action will require further investigations to indeed settle this phenomenon.

Glutamate Receptors

Glutamate receptors mediate the majority of excitatory neurotransmission in the mammalian central nervous system. They are responsible for neuronal excitation and

play a key role in neural plasticity, neural development and neurodegeneration. Glutamate receptors are pharmacologically categorized into two distinct receptor families: ionotropic (iGluR) and metabotropic glutamate receptors (mGluR). The iGluRs are ligand gated ion channels, which are subdivided into N-methyl-D-aspartate (NMDA), and non-NMDA receptors with the latter being further divided into α -amino-3-hydroxy-5-methyl-4-isoxazolepropionate (AMPA) and kainate distinguishing subtypes (kainate receptors). Non-NMDA receptors are mostly permeable to Na^+ and K^+ , while NMDA receptors are selectively permeable to Na^+ and Ca^{+2} . Physiologically rapid glutamatergic neurotransmission is mediated by non-NMDA receptors. Mg^{+2} physiologically blocks NMDA receptor channels in a voltage-dependent manner. Due to this characteristic, Ca^{+2} influx increases in response to the increasing levels of membrane depolarization that occurs during high frequency synaptic activity and it is this Ca^{+2} that activates processes that are fundamental to long-term changes in synaptic strength. The mGluRs are coupled to GTP-binding proteins (G-proteins) that regulate the production of intracellular messengers, including phospholipase C (PLC) and adenylate cyclase activity. MGluRs can elicit both prolonged excitatory and inhibitory effects in the CNS. MGluRs are classified into three groups in accordance with their signal transduction mechanisms, sequence similarities, and agonist selectivity.

Ionotropic Glutamate Receptors

IGluRs are expressed throughout the central nervous system and function as cation-specific ion channels. IGluR subunits contain three transmembrane domains (TM1, TM3 and TM4) and a re-entrant membrane loop (TM2). The TM2 region, located

on the cytoplasmic side, lines the inner channel pore and determines distinct ion selectivity of the ion channel (Kunner et al., 1996). This presumed topology orientates the N-terminus extracellularly and C-terminus is found intracellularly (Wo and Oswald, 1994,1995).

NMDA, AMPA, and kainate receptor subunits are encoded by at least six gene families: three for NMDA, two for kainate and one for AMPA. Sequence similarity and, to a lesser extent, similar intron-exon structure, suggest a common evolutionary origin for iGluR genes (Suchanek *et al.*, 1995). Molecular cloning and expression studies have lead to the isolation of 14 different cDNAs: five kainate receptor subunits (KA1, KA2, GluR5-GluR7), five NMDA receptor subunits (NR1, NR2A-NR2D), and four AMPA receptor subunits (GluR1 GluR4). Each subunit is a glycosylated integral polypeptide and, with the exception of the NR2 subunit (1300 amino acid residues), is comprised of approximately 900 amino acids residues.

Non-NMDA Receptors

Non-NMDA receptors were first identified as receptors being preferentially activated by quisqualic or kainic acid. However, upon the synthesis of AMPA the term “quisqualate receptor” was replaced by “AMPA receptor”, due to quisqualic activation of metabotropic receptors. Cloning studies have indicated a very rich variety of subunits from which to construct AMPA/kainate receptors (Seeburg, 1993; Hollmann and Heinemann, 1994; Bettler and Mülle, 1995). A total of nine subunits, GluR1-GluR7 and KA1-2, have been identified and can exist in a variety of isoforms generated by alternative splicing.

AMPA receptors can exist as homo- or hetero-oligomers composed of GluR1-GluR4 subunits (Hollmann *et al.*, 1989). These subunits consist of approximately 900 amino acid residues with 68-73% amino acid sequence homology (Seeburg 1993). Like other ion-channels, combinatorial assembly of heteromeric receptors gives rise to extensive functional heterogeneity of receptor subtypes. In addition to this, genetic alterations also contribute to the structural and functional diversity seen among glutamate receptors. Molecular cloning of the AMPA receptor revealed a segment of 115 bp existed in one or two sequence versions, each differing in pharmacological and kinetic properties (Sommer *et al.*, 1990). This segment encodes 38 amino acid residues within the conserved receptor domain immediately preceding the TM4 and hence is probably located intracellularly (Sommer *et al.*, 1990). These versions were given the names, flip and flop, with flop being the dominant form in the adult brain. Both flip and flop configurations process similar sequences in their respective segments, differing in only a few amino acids (9-11). The two isoforms are found in different populations of neurons and are developmentally regulated. *In-situ* hybridization histochemistry revealed that embryonic brains predominantly expressing the flip version, while conversion to the flop form start around postnatal 8 and gradually increases reaching adult levels (55% to ~100%) by postnatal day 14.

In addition to splice variation, AMPA receptors undergo RNA editing, which introduces yet another realm of complexity to its functional properties. The best demonstration of this can be seen in the case of GluR2 subunit. Recombinant expression studies have shown that the GluR2 subunit is responsible for the low Ca^{+2} permeability found among heteromeric AMPA receptors containing this subunit. However,

heteromeric AMPA receptors assembled from the GluR1/-3/-4 subunits show a significant permeability to Ca^{+2} . This discrepancy can be mapped to a single residue in the TM2 domain. This amino acid is the product of an RNA editing mechanism that converts the CAG (glutamine/Q) codon present in the GluR1/-3/-4 transcripts into the CGG (arginine/R) codon found in mature GluR2 mRNAs. This codon change is due to the conversion of adenosine (A)-to guanosine (G) and is developmentally regulated. Unedited GluR2 transcripts are not present in the adult brain, whereas the GluR1/-3/-4 subunits are not subject to RNA editing. This suggests that native AMPA receptors are heteromeric assemblies of unedited GluR1/-3/-4 subunits.

Like AMPA receptors, kainate-preferring receptors diversity is also mediated by RNA editing. As in the case of GluR2, GluR5 and GluR6 subtypes exhibit RNA editing at the Q/R site in the TM2 segment. But unlike GluR2, Q/R site editing is incomplete throughout development, and both edited and unedited versions coexist in the adult brain. GluR6 conversion Q to R has been shown to abolish Ca^{+2} permeability and is dominant in a heterologous receptor complex. Receptor complexity is further increased at two additional sites, located in TM1, which generate isoleucine (I) or valine (V) in one and tyrosine (Y) or cysteine (C) in the other. Unedited versions have V and T in their respective sites, while the edited version has I and Y. Editing at these positions modulate the effects of Q/R site Ca^{+2} flow, such that fully edited subunit exhibits no passage of the cation.

NMDA Receptors

NMDA receptors are composed of two types of subunits, NMDAR1 (NR1) and NMDAR2A to NMDAR2D (NR2A-D) (Moriyoshi *et al.*, 1991), while the identical gene

products of mouse NMDA receptor channels are GluR ζ and GluR ϵ (Ikeda *et al.*, 1992). In 1991, Moriyoshi *et al.* reported that, when expressed in *Xenopus* oocytes, the NR1 subunit demonstrated properties characteristic of native NMDA receptors. However, when the NR1 subunit was expressed in a mammalian expression system, no functional channels were formed (Chazot *et al.*, 1992) suggesting the requirement of an additional subunit. It was later determined that co-expression of NR2 subunits with NR1 enhances the expression of functional NMDA receptors in oocytes (Ishii *et al.*, 1993), with NR1 serving as the fundamental subunit and NR2 having a modulatory role (Seeburg, 1993). Due to the fundamental role of NR1, it is found ubiquitously throughout the brain, while NR2 subunits displays distinct regional and developmentally regulated expression patterns. Furthermore, pharmacological evidence indicate that NMDA receptors can function as heteromeric assemblies composed of multiple NR1 subunits in combination with two different isoforms of NR2 (Wafford *et al.*, 1993; Chazot *et al.*, 1994), thus creating pharmacologic diversity among NMDA receptors in the CNS.

In addition to the heterogeneous makeup, functional diversity of NMDA receptors is enhanced by alternative splicing of the NR1 gene, resulting in eight different splice variants. The NR1 subunit gene has a total of 22 exons, three (exons 5, 21 and 22) of which undergo alternative splicing. Exon 5 encodes a splice cassette of 21 amino acid (N1), which is part of the amino-terminal domain, whereas exons 21 and 22 encode two independent consecutive splice cassettes of 37 (C1) and 38 (C2) amino acids, which are found in the carboxyl-terminal domain (Sugihara *et al.*, 1992). These variants differ in their properties and are differentially localized in both the adult and developing animal.

As earlier described, the NMDA receptor is physiologically distinct from other glutamate receptors in its ability to mediate excitatory neurotransmission in many central synapses. It has a high permeability to Ca^{+2} and is blocked in a voltage-dependent manner by Mg^{+2} . Due to these properties, the NMDA receptor serves as a molecular apparatus that can detect the coincidence of presynaptic activity and postsynaptic depolarization at the synapse. In response, it injects the postsynaptic cell with a sufficient amount of the second messenger ion, Ca^{+2} , in turn initiating plastic changes in the strength of synaptic connection. An asparagine (N) residue governs both Ca^{+2} permeability and a lesser degree of Mg^{+2} block in both NR1 and NR2 subunits (Burnashev *et al.*, 1992c; Mori *et al.*, 1992). The degree of Mg^{+2} block is also dependent on the particular NR2 subunit coexpressed with NR1.

In addition to the voltage-sensitive Mg^{+2} block, NMDA receptors are susceptible to various endogenous and exogenous allosteric modulators. NMDA receptor activation requires glycine bound to a distinct strychnine-insensitive coagonist site. Though found on separate subunits, the glutamate and glycine sites reciprocally enhance each others affinity for binding to the NMDA receptor. Other modulatory sites include protons polyamines, redox, nitric oxide and zinc, all of which have relative affinities that are subunit and splice variant dependent.

Metabotropic Glutamate Receptors

mGluRs are G-protein coupled receptors, which modulate intracellular secondary messengers in the quest for achieving neuronal excitability and synaptic plasticity (Kano and Kato, 1987). The mGluR family is made up of 8 different subtypes, mGluR1-mGluR8, all sharing more than 40% homology. Subtypes are classified into three

subgroups (groups I, II, and III) on the basis of their amino acids sequence homology. Group I consists of mGluR1 and mGluR5; group II consists of mGluR2 and mGluR3; and group III consists of mGluR4, mGluR6 mGluR7 and mGluR8 (Pin and Duvoisin, 1995). mGluRs of the same subgroups have similar transduction mechanisms. Group I activation stimulates PLC and the subsequent inositol-1, 4,5-triphosphate (IP₃) production initiates Ca⁺² release from intracellular stores (Masu *et al.*, 1991). Groups II and III are negatively coupled to adenylyl cyclase (Tanabe *et al.*, 1992).

Mechanisms of Excitotoxic Neuronal Death

Excitotoxicity is defined as the ability of L-glutamate and structurally related excitatory amino acids to elicit neuronal destruction under certain conditions (Olney, 1978). This idea was based on the work of Lucas and Newhouse, who first described the neurotoxic effects of monosodium glutamate on the retina of the mouse (Lucas and Newhouse, 1957). Also contributing to this idea, Curtis *et al.* (1959) reported that amino acids had a neuroexcitatory effect in spinal neurons of the rat. Ten years later Olney extended these findings to the brain and spinal cord (Olney, 1969) and to primates (Olney and Sharpe, 1969). In 1978, Olney described the toxicity of glutamate as being a direct consequence of its interaction with receptors that mediate its excitatory effects on neurons and christened this phenomenon “excitotoxicity” (Olney, 1978).

Glutamate is the principle excitatory neurotransmitter found, in millimolar concentrations, at the majority of all synapses throughout the mammalian brain and spinal cord (Cotman, 1996). During normal physiologic process, glutamate is released from glutamatergic nerve terminals in response to depolarization, crosses the synaptic cleft, and acts on its respective receptors. Once activated, these receptors, acting as

ligand gated ion channels, result in further depolarization and neuronal excitation. This activation of excitatory amino acid receptors is transitory under normal conditions. Once depolarization reaches a certain threshold, a train of action potentials is generated.

Recent evidence has shown that excitotoxicity directly contributes to the pathogenesis of several human neurological disorders induced by various insults including hypoxia-ischemia, hypoglycemia, sustained epilepsy, and adult-onset neurodegenerative diseases (Meldrum, 1985). Because excitotoxicity has involvement in a number of human ailments, researchers are actively exploring and characterizing this phenomenon with hopes of finding a therapeutic utility applicable in clinical medicine.

In-vivo studies provided a basic understanding of excitotoxicity (McGreer and McGreer, 1982). It was reported that high systemic doses of glutamate resulted in pathological changes in the circumventricular regions of young rodent or monkey brains (Olney, 1969). Using electron microscopy, they noted an acute swelling of neuronal cell bodies and dendrites following a 30-minute exposure of glutamate. This dendrosomatotoxic swelling was followed by degeneration of intracellular organelles and nuclear pyknosis with the cell, eventually becoming necrotic and undergoing phagocytosis by macrophages.

Research in this field has since utilized various *in-vitro* preparations including primary and immortal cell culture, tissue culture, and brain slices. These simplified models not only produced results consistent with *in-vivo* methods of earlier work, but also has provided additional information on the underlying mechanisms otherwise unknown (Choi, 1992). It should be noted that variations in the nature of excitotoxicity

exist depending on the neuronal preparation used, leaving additional uncertainties in the precise mechanism.

During normal synaptic functioning, glutamate's excitatory effect is rapidly terminated due to its removal from the synapse by glutamate uptake systems found both in glial cells and nerve terminals. This function is dependent on specific transporter proteins, EAAT-1 to EAAT-4, which co-transport 3 Na⁺ ions accompanied with 1 glutamate molecule coupled to the counter-transport of 1 K⁺ ion. This process is indirectly driven by Na⁺/K⁺ ATPase, which requires approximately 60% of cellular ATP to maintain transmembrane electrochemical gradient. The efficiency of this process enables glutamate to be concentrated in the intracellular compartment up to 10,000-fold with respect to the extracellular milieu (~1μM). A major consequence of acute neurodegenerative diseases is the reduction of oxygen or glucose availability required for proper Na⁺/K⁺ ATPase functioning. This results in prolonged depolarization increasing synaptic glutamate release and reverses the mode of glutamate transporter function.

Not all neurons are susceptible to glutamate-induced excitotoxicity. Cerebellar granule neurons cultured in physiologic salt solution at 37°C, exposed to 300μM glutamate, did not exhibit excitotoxicity indicating their ability to maintain ionic homeostasis during ion flux induced by agonist stimulation (Berman and Murray, 1996). However, the removal of Mg⁺² from the culture medium did promote glutamate toxicity. Excitotoxicity also occurred when neuronal energy reserves were depleted or by K⁺ or veratridine depolarization (Schramm et al., 1990). This indicates that cerebellar granule cell excitotoxicity occurs only in the presence of an independent depolarizing stimulus capable of releasing the voltage-dependent Mg⁺² blockade of the NMDA receptor. This

demonstrates the importance of a neuron's ability to maintain ionic homeostasis to ensure its own survival.

Excitotoxic neuronal death is mediated by the prolonged depolarization of neurons, changes in intracellular Ca^{+2} concentrations, and the activation of enzymatic and nuclear mechanisms responsible for death (Choi, 1988). Classical excitotoxicity is achieved due to elevated levels of extracellular glutamate producing persistent depolarization of the neuron. Upon a brief, yet intense exposure of glutamate, the influx of Na^{+} accompanied with Cl^{-} and water occurs (Rothman, 1985). This is marked by the expansion of cell volume, which alters membrane permeability thus compromising homeostasis. This initial event can be completely reversible if the glutamate concentration or exposure duration is limited. The extent of swelling *in vivo* is less than that observed *in vitro* due to the open architecture of cell culture causing exaggeration of cell volume expansion.

The second, more delayed, excitotoxic event is dependent on extracellular Ca^{+2} levels and is mediated by both the excessive influx of this cation and its release from intracellular stores. The principle sources of elevated intracellular free Ca^{+2} are entry through voltage-dependent calcium channels and, in the presence of glutamate, through the opening of ligand-gated channels resultant of glutamate activation. Intracellular Ca^{+2} concentrations are also increased due to the impaired activity of the membrane $\text{Na}^{+}/\text{Ca}^{+2}$ exchanger, whose electrochemical driving force is decreased by depolarization (Koch and Barish, 1994). Additional evidence has suggested that the mitochondrial uptake of Ca^{+2} plays a significant role in glutamate-induced neurotoxicity (Stout et al., 1998; Nicholls and Budd, 1998). It was reported that an excessive increase in mitochondrial Ca^{+2} results

in cellular death by ATP depletion (Gunter and Gunter, 1994), mitochondrial membrane depolarization (White and Reynolds, 1996) and generation of reactive oxygen free radicals (White and Reynolds, 1996). Free radical attack on the mitochondria compromises energy production within the cell impairing Ca^{+2} extrusion and sequestration mechanisms (Montalet *et al.*, 1996). These Ca^{+2} -dependent events are known as, Ca^{+2} overload. This hypothesis suggests that neurodegeneration is a function of the quantity of Ca^{+2} that enters the cell (Manev *et al.* 1989). Choi and colleagues also showed that in cortical neurons exposed to glutamate (Choi *et al.*, 1989) or anoxia (Goldberg *et al.*, 1989), Ca^{+2} measurements are correlated precisely with cell death, which further supports this hypothesis.

Ca^{+2} overload can be divided into three-stage process: induction, amplification, and expression (Choi, 1990). Induction occurs upon the glutamate activation of its neuronal receptors, which initiates the development of the injury. This is noted by an increase in cytoplasmic Na^{+} , Cl^{-} , water, IP_3 and diacylglycerol, which are all components needed to trigger subsequent events. Following the induction of glutamate toxicity, several events occur that may amplify these intracellular derangements. These may include, Ca^{+2} release from intracellular stores, activation of certain enzymes including C-kinases, calmodulin-regulated enzymes, calpains, and phospholipases. These events, all acting in concert, may lead to lasting enhancement of excitatory synaptic efficacy and circuit excitability while altering neuronal Ca^{+2} homeostasis. The sustained elevation in intracellular Ca^{+2} sets the stage for the triggering of several destructive cascades, which bear full responsibility for neuronal degeneration. These specific cascades have been hypothesized to share origins of Ca^{+2} overload (Choi, 1992). One class of expression

cascades may initiate the Ca^{+2} -activated catabolic enzymes. Calpain I, a Ca^{+2} -activated neutral protease, is directly linked to glutamate receptors in rat hippocampus and can degrade major neuronal structural proteins (Siman, Noszek, and Kegerise, 1989). Increased cytosolic Ca^{+2} levels also activate phospholipases, which are capable of breaking down of the cell membrane and liberating arachidonic acid, and endonucleases capable of degrading genomic DNA (Choi, 1992).

Another class of destructive expression cascades involves reactive oxygen free radicals. These reactive molecules initiate a plethora of destructive processes, one including lipid peroxidation (Braugher and Hall, 1989; Siesjo, 1989). Once formed, these oxygen free radicals promoted further glutamate release attenuating additional excitotoxic injury (Pellegrini-Giampietro, Cherici, Alesiani, Carla, and Moroni, 1988).

Sodium Channels

Sodium channels are transmembrane proteins responsible for the voltage-dependent increase in sodium conductance that produces action potentials in excitable cells (Hodgkin and Huxley, 1952). Using voltage clamp techniques, Hodgkin and Huxley defined three key features characterizing sodium channels: voltage-dependent activation, rapid inactivation, and selective ion conductance (Hodgkin and Huxley, 1952). Sodium channels consist of a large pore forming α subunit (240-280 kDa) noncovalently associated to smaller auxiliary subunits: $\beta 1$, $\beta 2$, and $\beta 3$ (Catterall, 1992). Sodium channels in the mammalian brain exist as a heterotrimeric complex consisting of an α (260 kDa), $\beta 1$ (36 kDa), and a disulfide linked $\beta 2$ (33kDa) subunit (Catterall, 1992; Barchi, 1988; Hartshorne and Catterall, 1992). The α subunit consists of four homologous domains (I-IV) with each domain containing six transmembrane segments,

S1-S6, and one reentrant segment, SS1/SS2. The reentrant segment, SS1/SS2, is connected by internal and external polypeptide loops (Noda *et al.*, 1986). The voltage sensors are located in the positively charged S4 segment and initiate the voltage dependent activation of sodium channels by moving outward under the influence of the electric field (Armstrong, 1981). Inactivation is controlled by the short intracellular loop connecting domains III and IV (Stuhmer *et al.*, 1989). The SS1/SS2 segment forms the ion selectivity filter and the outer region of the pore (Heinemann *et al.*, 1992).

Neurotoxin Binding Sites

Radiolabeled neurotoxin assays uncovered at least six distinct neurotoxin-binding sites associated with the sodium channel (Catterall, 1977 and 1980). Neurotoxin binding generally alters ion permeation and/or voltage-dependent gating and can be classified as the following: pore-blocking toxins, toxins that affect gating from membrane-embedded receptor sites and toxins that affect gating from extracellular receptor sites (Catterall, 1980 and 2000).

Receptor site 1 on the sodium channel is occupied by the water-soluble heterocyclic guanidines, tetrodotoxin (TTX) and saxitoxin (STX) and the peptidic μ -contoxins. TTX is isolated from the tissue of at least 40 species of puffer fish (Fuhrman F.A., 1967) and can also be found in mollusks, octopus, crabs, and Central American frogs (Catterall 2000). Binding of these toxins has been shown to block sodium conductance (Hille, 1966; Narahashi, 1974). Upon binding to receptor site 1, TTX enters the extracellular opening of the transmembrane pore, thus preventing access of transported monovalent cation to the cation pore.

Various toxins including, lipid-soluble grayanotoxins, veratridine, acotinine, and batrachotoxin bind to neurotoxin intramembrane receptor site 2, which alters voltage-dependent gating. These toxins bind preferentially to the activated state of sodium channels, which causes a persistent activation at resting membrane potentials. It is suggested that the block of inactivation is due to their interaction with IVS6 transmembrane segment that is required for fast inactivation.

Having similar effects of site 2 neurotoxins, the lipid-soluble brevetoxins and ciguatoxins bind to neurotoxin receptor site 5 and cause a shift in activation to a more negative membrane potential and a block of inactivation (Benoit *et al.*, 1986; Huang *et al.*, 1985). Transmembrane segments IS6 and IVS5 are both involved in the formation of receptor site 5.

The polypeptide toxins, α -scorpion toxins, sea-anemone toxins and some spider toxins act on the extracellular neurotoxin receptor site 3. Upon binding, these toxins slow or block sodium channel inactivation. The binding affinity of this group of toxins is decreased by depolarization on rat brain sodium channels (Catterall, 1977; Couraud, 1978). Because the voltage dependence of neurotoxin binding correlates closely with the voltage dependence of channel activation, implies that membrane potential affects the structure of receptor site 3 on rat brain sodium channels. This suggests that this region of the channel is important for coupling of activation and inactivation and toxin binding prevents the conformational change required for fast inactivation (Catterall, 1979).

The polypeptide toxin conotoxin-TxVIA purified from the venom of the cone snail *Conus textile* led to the discovery of neurotoxin site 6. Conotoxin -TxVIA causes a

specific inhibition of sodium current inactivation by producing a marked prolongation of action potential.

The β -scorpion toxins act on neurotoxin receptor site 4. β -scorpion toxins induce both a shift in the voltage dependence of sodium channel activation in the hyperpolarizing direction and a reduction of the peak sodium current amplitude. The voltage dependence of activation of neuronal sodium channels is modified by β -scorpion toxin only after a strong depolarizing prepulse. This suggests that the interaction of the toxin with its receptor site must be dependent on the activated conformational state of the toxin receptor site.

Antillatoxin Induced Neurotoxicity

Antillatoxin, a secondary metabolite produced by *Lyngbya majuscula*, has been shown to induce distinct temporal patterns of NMDA receptor-mediated neurotoxicity in CGCs (Berman *et al.*, 1999). It was reported that antillatoxin had an acute concentration-dependent neurotoxic effect in rat cerebellar granule neurons 10-12 days *in-vitro*. The neurons were exposed to antillatoxin for 2 hours at which time media was collected and replaced by the original growth medium for additional profiling of neurotoxic activity. Neurotoxicity was quantified by the release of lactate dehydrogenase (LDH) in the culture media as determined spectrophotometrically (Koh and Choi, 1987). The LC_{50} value, after 2-hour exposure time, for the antillatoxin-stimulated LDH efflux was 20.1 ± 6.4 nM. Neuronal morphology consisted of swelling of neuronal somata, thinning of neurites and blebbing of neurite membranes, all signs of cytotoxicity. The morphological changes were noted within the first 5 minutes and lasted throughout the exposure period.

Antillatoxin's excitotoxic effect was mediated through NMDA receptor-dependent mechanisms. This was determined by exposing the neurons to both, 100 nM antillatoxin and 100 μ M dextrorphan or 1 μ M (+)-5-methyl-10,11-dihydro-5H-dibenzo[a,d]cyclohepten-5,10-imine maleate (MK-801), NMDA receptor antagonists. Both dextrorphan and MK-801 afforded neuroprotection in the acute and delayed antillatoxin-induced neurotoxicity. However, there was no significant decrease in toxicity when the NMDA receptor antagonists were only present in the 22-hour post-exposure period.

Li *et al.* later hypothesized that antillatoxin's neurotoxic effect was dependent on voltage-gated Na⁺ channels (Li *et al.*, 2001). Neurons co-exposed to Antillatoxin (100nM) and TTX (1 μ M) resulted in a complete elimination of the ATX-induced neurotoxicity. Also supporting this hypothesis, Li *et al.* showed that antillatoxin caused a concentration-dependent increase in neuronal loss in neuro-2a cells treated with ouabain and veratridine. They also found that Antillatoxin produced a TTX sensitive Ca⁺² influx in CGCs similar to known sodium channel activators.

Further elucidating antillatoxin's interaction with voltage-dependent Na⁺ channels, Li *et al.* (2001) assayed tritiated batrachotoxin A 20- α -benzoate (³H]BTX) binding in the presence and absence of antillatoxin, in an attempt to detect any allosteric coupling between the two neurotoxin binding sites. BTX binds preferentially to site 2 of the active state of voltage-dependent Na⁺ channels and is sensitive to conformational changes induced by the binding of toxins to other sites on the α subunit (Catterall *et al.*, 1981). Antillatoxin produced a concentration-dependent stimulation of [³H]BTX-specific binding, which was synergistically augmented by brevetoxin (PbTx-1). Antillatoxin

increased [^3H]BTX binding 4.8-fold while PbTx-1 produced a 2-fold stimulation. The combination of antillatoxin and PbTx-1 increased specific binding 16.6-fold in a synergistic manner. Antillatoxin's allosteric effects were further characterized by evaluating the combination of maximally effective concentrations of sea anemone toxin and deltamethrin with antillatoxin. Sea anemone toxin displayed a 1.8-fold increase in [^3H]BTX binding, and in the presence of antillatoxin enhanced binding to 4.6-fold. This demonstrated a lack of synergism between antillatoxin and neurotoxin site 3. Deltamethrin in the presence of antillatoxin increases specific binding to 5.2-fold stimulation, which also indicated a lack of synergistic activity. These results suggest that antillatoxin, sea anemone and deltamethrin all act at distinct sites that are not allosterically coupled. However, PbTx-1 data did exhibit a synergistic effect with antillatoxin suggesting antillatoxin's binding site could be allosterically coupled and /or topologically close to neurotoxin site 5.

In conjunction to antillatoxin's enhancement of [^3H]BTX-specific binding, Li *et al.* (2001) also reported that antillatoxin stimulated a, TTX-sensitive, $^{22}\text{Na}^+$ influx in intact CGCs with an EC_{50} of $98.2 \pm 12. \text{nM}$. This work provides strong support for the hypothesis that antillatoxin is an activator of voltage-gated sodium channels.

**The Autocrine Excitotoxicity Of Antillatoxin, A Novel Lipopeptide Derived
From The Pantropical Marine Cyanobacterium *Lyngbya majuscula***

Materials

Acetonitrile, ethanethiol, and OPD were purchased from Fisher Scientific (Norcross, GA). Tetrodotoxin was purchased from Sankyo (Tokyo, Japan). Trypsin, basal medium Eagle's, gentamycin, heat-inactivated FBS, soybean trypsin inhibitor, and DNase were obtained from Atlanta Biologicals (Norcross, GA). Poly-l-lysine and cytosine arabinoside were obtained from Sigma Chemical Co (St. Louis, MO). Fluo-3 AM and Pluronic acid were obtained from Molecular Probes (Eugene, OR, U.S.A.). ATX was either authentic natural (–)-antillatoxin, isolated as described, or synthetic (–)-antillatoxin prepared as published. Tetanus toxin (TT) was purchased from List Biologicals (Campbell, CA, U.S.A.).

Cerebellar Granule Cell Culture

Primary cultures of CGNs were obtained from 8-day-old Sprague-Dawley rats as previously described (Berman and Murray, 1996). Isolated cerebella were stripped of meninges, minced by mild trituration with a Pasteur pipette, and treated with trypsin for 15 min at 37°C. Granule cells were then dissociated by two successive trituration and sedimentation steps in soybean trypsin inhibitor- and DNase-containing isolation buffer, centrifuged, and resuspended in basal Eagle's medium with Earle's salts containing 10%

heat-inactivated FBS, 2 mM glutamine, 25 mM KCl, and 100 µg/ml gentamicin. The neurons were plated onto poly-L-lysine (mw = 393,000)-coated 6-well (35-mm) culture dishes (Fisher) at a density of $\sim 2.5 \times 10^6$ cells/well and incubated at 37°C in a 5% CO₂/95% humidity atmosphere. Cytosine arabinoside (10 µM) was added after 18 to 24 h to inhibit replication of non-neuronal cells. Cells were fed after 7 to 8 days in culture (DIC) with 50 µl/ml of a 25 mg/ml dextrose solution.

Cytotoxicity Assays

CGNs were used for toxicologic assays at 11 to 13 days in culture (DIC). All assays were carried out in 0.1% DMSO. DMSO alone had no effect on neurons at concentrations as high as 1%. Growth medium was collected and saved, and the neurons washed twice in 1 ml of Locke's incubation buffer containing 154 mM NaCl, 5.6 mM KCl, 1.0 mM MgCl₂, 2.3 mM CaCl₂, 8.6 mM HEPES, 5.6 mM glucose, and 0.1 mM glycine, pH 7.4. The neurons were then exposed to ATX in the presence or absence of antagonist compounds in 0.5 ml of Locke's buffer for 2 h at 22°C. At the termination of ATX exposure, the incubation medium was collected for later analysis of lactate dehydrogenase (LDH) activity, and the neurons were washed twice in 1 ml of fresh Locke's followed by replacement with 1 ml of the previously collected growth medium that had been filtered and supplemented with 25 mg/ml sucrose. The cell cultures were returned to the 37°C incubator. At 24 h after ATX exposure, growth medium was collected and saved for analysis of LDH activity. LDH activity was assayed according to the method of Koh and Choi (1987).

Neuronal injury was assessed morphologically by exposing CGNs for 5 min to the vital dye fluorescein diacetate (5 $\mu\text{g/ml}$). The neurons were photographed at 400 \times magnification using an Olympus model IX50 inverted microscope equipped with fluorescence optics. Under fluorescence, somata and neurites of nonintoxicated neurons stain bright green, whereas injured neurons stain weakly due to a reduced ability to accumulate and hydrolyze the dye to the UV-excitable fluorescein molecule.

Measurement of Excitatory Amino Acid Release

Exposure conditions in excitatory amino acid (EAA) release studies were identical with those used in excitotoxicity assays. The exposure buffer was collected at specific time points, derivatized with *o*-phthaldialdehyde (OPD), and assayed for EAA content by HPLC according to the method of Hill et al. (1979) with modifications. The derivatization reaction was initiated by the addition of 80 μl of borate buffer (saturated solution, pH 9.5), 200 μl of 100% methanol, and 40 μl of an OPD solution (50 mg in 4.5 ml of 100% methanol, 0.5 ml of borate buffer, 50 μl of ethanethiol) to 80- μl aliquots of exposure buffer. Twenty microliters of the derivatized sample was injected by autosampler (Beckman 508 with Gold Nouveau software) onto a reverse-phase column (250 \times 4.5 mm i.d.; Supelco LC-18) with guard column (15 \times 4.6 mm i.d.), both packed with 5- μm particles. The effluent was monitored fluorometrically (model; FS-970 Kratos) with the following settings for detection: excitation monochromometer at 229 nm, a 470-nm emission cutoff filter, a 1.0- μA full-scale range setting with a time constant of 0.5 s, and a sensitivity setting of 5.42 units. The mobile phase was 0.0125 M Na_2HPO_4 (pH 7.2) and acetonitrile at a flow rate of 1 ml/min in a gradient from 9 to 24% over 15 min

followed by an increase to 49% over 20 min and then an immediate reduction to 9% and hold for 6 min. L-Aspartate and L-glutamate were detected at retention times of 8.2 and 10.6 min, respectively.

Intracellular Ca²⁺ Monitoring

CGNs grown in 96-well plates were used for intracellular Ca²⁺ ([Ca²⁺]_i) measurements at 10-13 DIC. The growth medium was removed and replaced with dye loading medium (100 µl/well) containing 4 µM fluo-3 AM and 0.04% pluronic acid in Locke's buffer (154 mM NaCl, 5.6 mM KCl, 1.0 mM MgCl₂, 2.3 mM CaCl₂, 8.6 mM HEPES, 5.6 mM glucose, and 0.1 mM glycine, pH 7.4). Fluo-3 AM is taken up by cells and entrapped intracellularly after hydrolysis to fluo-3 by cell esterases. Preliminary experiments determined that dye loading was optimal after 1 h at 37°C. After the 1-h incubation in dye loading medium, the neurons were washed four times in fresh Locke's buffer (200 µl/well, 22°C) using an automated cell washer (Labsystems, Helsinki, Finland) and transferred to the FLIPR incubation chamber. The final volume of Locke's buffer in each well was 100 µl.

FLIPR operates by illuminating the bottom of a 96-well microplate with an argon laser and measuring the fluorescence emissions from cell-permeant dyes in all 96 wells simultaneously using a cooled CCD camera (Schroeder and Neagle, 1996). Moreover, this instrument is equipped with an automated 96-well pipettor, which can be programmed to deliver precise quantities of solutions simultaneously to all 96 culture wells from two separate 96-well source plates. In all experiments, antagonist compounds were added to the neurons from one source plate in a 50 µl volume and at a rate of 10 µl/s

3 min prior to the addition of a 50 μ l volume of PbTx-1 added from the second source plate at 25 μ l/s, yielding a final volume of 200 μ l/culture well and 1% dimethyl sulfoxide concentration. Neurons were excited by the 488-nm line of the argon laser, and Ca^{2+} -bound fluo-3 emission in the 500-to 560-nm range was recorded with the CCD camera shutter speed set at 0.4 s. Prior to each experiment, average baseline fluorescence was set between 10,000 and 15,000 U by adjusting the power output of the laser. Fluorescence readings were taken once every 2 s for 10 s prior to antagonist additions, every 10 s during the 3 min prior to PbTx-1 addition, then once per s for 75 s following PbTx-1 exposure and every 30 s thereafter to the programmed termination of the experiment. The FLIPR software saved the fluo-3 fluorescence versus time data automatically. Background fluorescence was automatically subtracted from all fluo-3 fluorescence measurements.

Quantification of Results

For each brevetoxin or antagonist concentration used in neurotoxicity assays, total LDH activity in triplicate plates was determined, the results were averaged, and LDH efflux in excess of control sister cultures run in parallel was determined. The LDH efflux value obtained from exposure buffer collected at 2 h was added to that obtained from media at 24 h to derive a measure of the cumulative change in LDH activity occurring over time. Nonlinear regression analysis and graphs were generated using GraphPAD Prism software (San Diego, CA). EC_{50} values for brevetoxin neurotoxicity and glutamate receptor antagonist neuroprotection were determined by nonlinear least-squares fitting of a logistic equation to concentration-response data.

The fluorescent detection of L-aspartate and L-glutamate derivatives was recorded and integrated using Beckman Gold Nouveau software. EAA concentrations in exposure buffer were determined by comparing unknown peak area-under-the-curve values with known external amino acid standards.

LDH efflux, Fluo-3 fluorescence, and EAA release data were analyzed and graphs generated with Graph-Pad Prism (San Diego, CA, U.S.A.) software. The EC₅₀ value for PbTx-1-stimulated increases in fluo-3 fluorescence was determined by nonlinear least-squares fitting of a logistic equation to the PbTx-1 concentration versus fluo-3 fluorescence area under the curve data.

Results

Our lab has previously demonstrated that a 2-hour exposure to antillatoxin induces an acute concentration-dependent neurotoxic response in 12 DIC CGNs in a physiologic buffer at 22° (Berman *et al.*, 1999). The reported EC₅₀ for 24-hour LDH accumulation was 20 ± 6.4 nM. Control neurons remained unaffected by these experimental manipulations. In the present report, identical exposure conditions were utilized and neuronal injury was assessed by measuring LDH activity in the exposure buffer after 2 hours and in conditioned growth medium at 22 hours after the termination of the excitotoxin exposure. As shown in figure 1, ATX produced a concentration-dependent increase in LDH activity. EC₅₀ values were 18.2 ± 1.6 nM and 28.3 ± 0.6 nM at 2 and 24 hours, respectively. Tetrodotoxin (TTX) was utilized to inhibit neuronal depolarization resulting from Na⁺ influx through voltage-dependent Na⁺ channels. We found that the coincubation of TTX (1 μM) with ATX during the 2-hour exposure period

completely eliminated ATX-induced neurotoxicity. These data support earlier work in our lab suggesting that ATX-induced neurotoxicity may depend on the activation of voltage-gated Na channels (Li *et al.* 2001). In further support of the idea that ATX may act as a Na⁺-channel toxin, we determined that 300 nM ATX induced a rapid change in membrane potential as measured by the relative change in DiBAC fluorescence (fig. 2). DiBAC, a bis-barbituric acid oxonol derivative, enters a depolarized cell where it binds to intracellular proteins or membranes and exhibit enhanced fluorescence. The change of relative fluorescence due to 300 nM ATX was comparable to that seen with 100 mM KCL, which suggests that ATX is a Na⁺ channel activator capable of completely depolarizing a cerebellar granule neuron (fig. 2).

Neuronal injury at 5, 30, and 120-minute time points were confirmed morphologically by assessing the ability of CGNs to accumulate the vital dye fluorescein diacetate and to hydrolyze it to fluorescein, which fluoresces green under ultraviolet light. As shown in Fig. 3, the somata and neurites of nonexposed control neurons stained intensely and maintained structural integrity, whereas CGNs exposed to ATX stained less intensely; had swollen, poorly defined somata; and demonstrated early signs of neurite membrane blebbing. This occurred in a concentration (not shown) and time dependent fashion.

Because CGNs are glutamatergic in nature, our hypothesis was that ATX, acting as an autocrine excitotoxic agent, depolarizes the neuron and, as a consequence, evokes the release of glutamate. This notion was based on the earlier finding that ATX causes NMDA receptor-mediated neurotoxicity in CGNs (Berman *et al.*, 1999) and that ATX is a potent sodium channel activator (Li *et al.*, 2001). In order to determine if ATX's

neurotoxicity was dependent on the release of glutamate, we exposed primary cultured CGN to ATX and then the incubation buffers were assayed for the presence of glutamate. As shown in figure 4, 100 nM antillatoxin induced a rapid increase in extracellular glutamate levels within the first 15 minutes of exposure, then increased more slowly before peaking at 30 minutes, after which the signal remained steady over the 1.5-hour time course. From this, we determined that an incubation time of 30 minutes would allow ATX enough time to evoke significant glutamate release in CGNs.

As indicated in figure 5, neurons exposed to increasing concentrations of ATX produced a (TTX sensitive) concentration-dependent increase in extracellular glutamate levels ($EC_{50} = 35.0 \pm 1.1$ nM). The amount of glutamate release in response to ATX correlates reasonably well with the degree of neuronal injury ($r^2 = .9482$)(fig. 6).

The rate and concentration dependence of the increase in $[Ca^{+2}]_i$ stimulated by ATX were examined in fluo-3-loaded CGNs. ATX produced a rapid and concentration-dependent increase in $[Ca^{+2}]_i$. At 100 nM ATX, fluo-3 fluorescence peaked within the first 250-300 seconds and then remained at a plateau level for the duration of the experiment (fig. 7A). Non-linear regression analysis of the concentration dependence of the ATX-evoked integrated fluo-3 response indicated that the EC_{50} for the ATX-stimulated increases in $[Ca^{+2}]_i$ was 55.6 nM (fig. 7B). This EC_{50} value correlates with the EC_{50} value for LDH efflux in CGN exposed 30 minutes to ATX ($r^2 = .8475$) (fig. 8).

To ascertain the ATX-stimulated glutamate release pathways, we conducted a pharmacological analysis of the response to a fixed concentration of 100 nM ATX at a time point of 30 minutes (fig. 9A). When neurons were pre-incubated for 1-hour with 200 μ M L-trans-pyrrolidine-2,4 dicarboxylic acid (PDA), a competitive and transportable

inhibitor of the high affinity glutamate transporter, glutamate concentration was modestly reduced to 72.2% of the control value. Inasmuch as significant neuronal swelling was apparent within the first five minutes of ATX exposure, we also investigated the extent to which osmotically driven swelling contributed to glutamate efflux. We found that when 100 mM sucrose was added to the exposure buffer, glutamate concentrations were reduced to 52.8 % of the control value. To determine the role of Ca^{+2} - dependent exocytotic glutamate release in response to ATX we used tetanus toxin (TT), an inhibitor of this mode of glutamate release. A 24-hour pretreatment of the neurons with 37.5 nM TT significantly decreased glutamate efflux to 35.0 % of control values. From these results, it appears that ATX-exposed primary cultured CGN release glutamate by three primary routes: reversal of the Na-dependent glutamate transporter, Ca^{+2} - dependent exocytotic release and via osmotically driven swelling with attendant glutamate release.

Given the reductions in extracellular glutamate concentrations that were produced by antagonist of the various glutamate efflux pathways, the extent to which these compounds protect CGN from the cytotoxicity resulting from a 2-hour exposure to 100 nM ATX was investigated (fig 9B). With the exception of the incubation time being 2-hours, exposure conditions were identical to those used in the glutamate release studies. Neuronal injury was greatly attenuated in ATX-exposed CGN by the presence of 100 mM sucrose. ATX-stimulated LDH efflux was reduced by 85.5 % and the neurons appeared morphologically normal at 2-hours. Neuronal injury was modestly attenuated by 200 μM PDA, which reduced LDH efflux by 35.8 %, whereas 37.5 nM TT offered virtually no protection against the ATX challenge.

Discussion

A primary aim of this study was to characterize ATX-induced neurotoxicity in cultured cerebellar granule neurons. Our model employs a physiologic media, which preserves normal cell signaling mechanisms. In a previous report, it was shown that ATX produced concentration-dependent cytotoxicity in CGNs (Berman *et al.*, 1999). This response was prevented by the non-competitive NMDA receptor antagonists, MK-801 and dextrorphan (Berman *et al.*, 1999). The present study extends those previous findings and examines the role of the release of endogenous glutamate in CGNs.

In the current report, we show that ATX produces a concentration-dependent glutamate efflux in cultured rat CGNs. Prevention of this response by TTX confirmed that ATX neurotoxicity is dependent on the activation of voltage-sensitive Na⁺ channels. This is in agreement with earlier work, which suggests that ATX is a Na⁺ channel activator (Li *et al.*, 2001). To further explore the role of ATX's interaction with voltage-gated Na⁺ channels, we monitored real-time alterations in membrane potential in DiBAC-loaded CGNs exposed to 300 nM ATX using FLIPR. This instrumentation permits the simultaneous measurement of fluorescence signals in a 96-well plate with a time domain of seconds. We determined that the relative change in membrane potential of CGNs exposed to 300 nM ATX was very close in magnitude to our positive control, 100 mM KCL. (At 20° C the Nernst equilibrium potential for 100mM KCL dissolve in Locke's buffer is -9.69 mV) These data not only support the idea of ATX being a Na⁺ channel activator, but also demonstrate ability to completely depolarize neurons.

Another type of Na⁺-channel activator are brevetoxins, a class of potent lipid-soluble polyether neurotoxins produced by the marine dinoflagellate *Karenia brevis*. Brevetoxins interact with neurotoxin site 5 on the α -subunit on the voltage-gated sodium channel. This interaction causes a shift in the voltage dependence of channel activation to more negative potentials and inhibits channel inactivation, thereby producing neuronal depolarization.

It has been reported that brevetoxin-mediated neuronal depolarization results in acute neuronal injury and cell death. Coapplication of TTX or NMDA receptor antagonists prevents all neurotoxicity associated with brevetoxins (Berman and Murray, 1999). Brevetoxins stimulate the release of glutamate from CGNs indicating that the neurotoxicity of these marine toxins is mediated by NMDA receptors, which are activated indirectly as a consequence of brevetoxin activation of channels with attendant glutamate release. Therefore brevetoxin-induced neurotoxicity in CGNs is due to autocrine excitotoxic mechanisms.

Our lab has also investigated the toxicologic mechanisms of another marine neurotoxin, domoic acid, which is a tricarboxylic amino acid produced by various species of marine diatom that causes severe neurologic dysfunction and necrosis in the brain (Berman and Murray, 1997). Domoate is also capable of producing an autocrine excitotoxicity in CGNs, which is mediated largely through NMDA receptors (Berman and Murray, 1997). However, unlike brevetoxins, domoate targets the AMPA/kainate receptor subtype. Activation of these receptors produces glutamate release with subsequent activation of NMDA receptors. It is reasonable to suggest that both brevetoxins and domoic acid produce autocrine excitotoxicity in CGNs.

ATX-mediated neurotoxicity resembles that of brevetoxin and domoic acid in that it may be prevented by coapplication of an NMDA receptor antagonist. Moreover, ATX-governed neurotoxicity is completely eliminated by TTX, which is similar brevetoxin-induced neurotoxicity. Li *et al.* (2001) has also shown that, like brevetoxins, ATX produces a (TTX-sensitive) increase in $[Ca^{+2}]_i$ in CGNs that may derive from activation of voltage-dependent Ca^{+2} channels, reverse mode of operation of the Na^+ / Ca^{+2} exchanger, and/or influx through NMDA receptors (Li *et al.*, 2001). It is noteworthy that we confirmed this $[Ca^{+2}]_i$ increase by monitoring fluo-3-loaded CGN exposed to various concentrations of ATX (fig. 7).

We hypothesized that ATX, acting as a Na^+ -channel activator, would cause an influx of Na^+ ions, in turn creating neuronal depolarization with attendant glutamate release and subsequent NMDA activation. In a number of reports, the neuronal release of glutamate resulting from depolarization or ischemia has been shown to occur by three primary mechanisms: Ca^{+2} -dependent vesicular release (Nicholls and Attwell, 1990), reversal of the high affinity Na^+ -coupled glutamate transporter (Longuemare and Swanson, 1995), and/or swelling-induced glutamate release (Kimmelberg *et al.*, 1990). The extent to which particular mechanism predominates depends upon factors that affect neuronal energetics and ion homeostasis (Nicholls, 1989; Nicholls and Attwell, 1990).

We investigated to which extent each of the glutamate release pathways contributed to the neurotoxic effects of ATX. We found that preventing the reversal of the high affinity Na^+ -coupled glutamate transporter attenuated ATX-evoked glutamate release in a manner commensurate with the corresponding reduction in cytotoxicity. However, inhibiting the Ca^{+2} -dependent vesicular release did provide a substantial

decrease in glutamate efflux, but no corresponding reduction in cytotoxicity was seen. Moreover, whereas hyperosmotic conditions completely eliminated the swelling-dependent release of LDH, a similar reduction in cytotoxicity did not occur.

The fact that sucrose protected CGNs against ATX-induced cytotoxicity (2-hours) but only offered a mild reduction of glutamate release indicates that the neurotoxic response is dependent on neuronal swelling. The neurotoxicity observed 22 hours later is most likely dependent on the release of glutamate with subsequent activation of NMDA receptors (Berman *et al.*, 1999). These findings are similar to those of Goldberg and Choi (1993), who have shown that inhibition of swelling in cortical neuron cultures during oxygen-deprivation protects against acute injury but not delayed neurodegeneration.

In conclusion we have shown that ATX stimulates a rapid and (TTX sensitive) concentration-dependent increase in extracellular glutamate, the magnitude of which correlates closely with the severity of neurotoxicity produced. ATX-mediated glutamate efflux is due to the magnitude of Na^+ influx, which occurs subsequent to activation of the voltage-sensitive Na^+ channel by ATX. This ATX-stimulated increase in extracellular glutamate occurs through three routes: Ca^{+2} -dependent vesicular release, reversal of the high affinity Na^+ -coupled glutamate transporter and swelling-induced glutamate release.

REFERENCES

- Armstrong, C. M. (1981). "Sodium channels and gating currents." *Physiol Rev.*, 61(3), 644-683.
- Baden, D. G. (1989). "Brevetoxins: unique polyether dinoflagellate toxins." *FASEB J.*, 3(7), 1807-1817.
- Barchi, R. L. (1988). "Probing the molecular structure of the voltage-dependent sodium channel." *Annu. Rev. Neurosci.*, 11, 455-495.
- Benoit, E., Legrand, A. M., and Dubois, J. M. (1986). "Effects of ciguatoxin on current and voltage clamped frog myelinated nerve fibre." *Toxicon*, 24(4), 357-364.
- Berman, F. W. and Murray, T. F. (1996). "Characterization of glutamate toxicity in cultured rat cerebellar granule neurons at reduced temperature." *J. Biochem. Toxicol.*, 11(3), 111-119.
- Berman, F. W. and Murray, T. F. (1997). "Domoic acid neurotoxicity in cultured cerebellar granule neurons is mediated predominantly by NMDA receptors that are activated as a consequence of excitatory amino acid release." *J. Neurochem.*, 69(2), 693-703.
- Berman, F. W., Gerwick, W. H., and Murray, T. F. (1999). "Antillatoxin and kalkitoxin, ichthyotoxins from the tropical cyanobacterium *Lyngbya majuscula*, induce distinct temporal patterns of NMDA receptor-mediated neurotoxicity." *Toxicon*, 37(11), 1645-1648.
- Berman, F. W. and Murray, T. F. (1999). "Brevetoxins cause acute excitotoxicity in primary cultures of rat cerebellar granule neurons." *J. Pharmacol. Exp. Ther.*, 290(1), 439-444.
- Berman, F. W. and Murray, T. F. (2000). "Brevetoxin-induced autocrine excitotoxicity is associated with manifold routes of Ca²⁺ influx." *J. Neurochem.*, 74(4), 1443-1451.
- Berman, F. W., LePage, K. T., and Murray, T. F. (2002). "Domoic acid neurotoxicity in cultured cerebellar granule neurons is controlled preferentially by the NMDA receptor Ca(2+) influx pathway." *Brain Res.*, 924(1), 20-29.
- Bettler, B. and Mülle, C. (1995). "Review: neurotransmitter receptors. II. AMPA and kainate receptors." *Neuropharmacology*, 34(2), 123-139.

- Braugher, J. M. and Hall, E. D. (1989). "Central nervous system trauma and stroke. I. Biochemical considerations for oxygen radical formation and lipid peroxidation." *Free Radic. Biol. Med.*, 6(3), 289-301.
- Burnashev, N., Schoepfer, R., Monyer, H., Ruppersberg, J. P., Gunther, W., Seeburg, P. H., and Sakmann, B. (1992). "Control by asparagine residues of calcium permeability and magnesium blockade in the NMDA receptor." *Science*, 257(5075), 1415-1419.
- Carmichael, W. W. (1992). "Cyanobacteria secondary metabolites--the cyanotoxins." *J. Appl. Bacteriol.*, 72(6), 445-459.
- Catterall, W. A. (1975). "Activation of the action potential Na^+ ionophore of cultured neuroblastoma cells by veratridine and batrachotoxin." *J. Biol. Chem.*, 250(11), 4053-4059.
- Catterall, W. A. (1977). "Activation of the action potential Na^+ ionophore by neurotoxins. An allosteric model." *J. Biol. Chem.*, 252(23), 8669-8676.
- Catterall, W. A., Morrow, C. S., and Hartshorne, R. P. (1979). "Neurotoxin binding to receptor sites associated with voltage-sensitive sodium channels in intact, lysed, and detergent-solubilized brain membranes." *J. Biol. Chem.*, 254(22), 11379-11387.
- Catterall, W. A. (1980). "Neurotoxins that act on voltage-sensitive sodium channels in excitable membranes." *Annu. Rev. Pharmacol. Toxicol.*, 20, 15-43.
- Catterall, W. A., Morrow, C. S., Daly, J. W., and Brown, G. B. (1981). "Binding of batrachotoxinin A 20-alpha-benzoate to a receptor site associated with sodium channels in synaptic nerve ending particles." *J. Biol. Chem.*, 256(17), 8922-8927.
- Catterall, W. A., Trainer, V., and Baden, D. G. (1992). "Molecular properties of the sodium channel: a receptor for multiple neurotoxins." *Bull. Soc. Pathol. Exot.*, 85(5 Pt 2), 481-485.
- Catterall, W. A. (2000). "From ionic currents to molecular mechanisms: the structure and function of voltage-gated sodium channels." *Neuron*, 26(1), 13-25.
- Chazot, P. L., Cik, M., and Stephenson, F. A. (1992). "Immunological detection of the NMDAR1 glutamate receptor subunit expressed in embryonic kidney 293 cells and in rat brain." *J. Neurochem.*, 59(3), 1176-1178.
- Chazot, P. L., Coleman, S. K., Cik, M., and Stephenson, F. A. (1994). "Molecular characterization of N-methyl-D-aspartate receptors expressed in mammalian cells yields evidence for the coexistence of three subunit types within a discrete receptor molecule." *J. Biol. Chem.*, 269(39), 24403-24409.

- Choi, D. W. (1988). "Glutamate neurotoxicity and diseases of the nervous system." *Neuron*, 1(8), 623-634.
- Choi, D. W. and Rothman, S. M. (1990). "The role of glutamate neurotoxicity in hypoxic-ischemic neuronal death." *Annu. Rev. Neurosci.*, 13, 171-182.
- Choi, D. W. (1992). "Excitotoxic cell death." *J. Neurobiol.*, 23(9), 1261-1276.
- Codd, G. A. (1984). "Toxins of freshwater cyanobacteria." *Microbiol. Sci.*, 1(2), 48-52.
- Couraud, F., Rochat, H., and Lissitzky, S. (1978). "Binding of scorpion and sea anemone neurotoxins to a common site related to the action potential Na^+ ionophore in neuroblastoma cells." *Biochem. Biophys. Res. Commun.*, 83(4), 1525-1530.
- Cox, J. A., Felder, C. C., and Henneberry, R. C. (1990). "Differential expression of excitatory amino acid receptor subtypes in cultured cerebellar neurons." *Neuron*, 4(6), 941-947.
- Curtis, D. R. and Watkins, J.C. (1963) Acidic amino acids with strong excitatory action. on mammalian neurons. *J. Physiol.* 66:1-14
- Fuhrman, F. A. (1967). "Tetrodotoxin. It is a powerful poison that is found in two almost totally unrelated kinds of animal: puffer fish and newts. It has been serving as a tool in nerve physiology and may provide a model for new local anesthetics." *Sci. Am.*, 217(2), 60-71.
- Goldberg, M. P. and Choi, D. W. (1990). "Intracellular free calcium increases in cultured cortical neurons deprived of oxygen and glucose." *Stroke*, 21(11 Suppl), III75-III77.
- Gunter, T. E., Gunter, K. K., Sheu, S. S., and Gavin, C. E. (1994). "Mitochondrial calcium transport: physiological and pathological relevance." *Am. J. Physiol*, 267(2 Pt 1), C313-C339.
- Hall, E. D. and Braughler, J. M. (1989). "Central nervous system trauma and stroke. II. Physiological and pharmacological evidence for involvement of oxygen radicals and lipid peroxidation." *Free Radic. Biol. Med.*, 6(3), 303-313.
- Hartley, D. M. and Choi, D. W. (1989). "Delayed rescue of N-methyl-D-aspartate receptor-mediated neuronal injury in cortical culture." *J. Pharmacol. Exp. Ther.*, 250(2), 752-758.
- Hartshorne, R. P. and Catterall, W. A. (1984). "The sodium channel from rat brain. Purification and subunit composition." *J. Biol. Chem.*, 259(3), 1667-1675.
- Heinemann, S. H. and Sigworth, F. J. (1989). "Estimation of Na^+ dwell time in the gramicidin A channel. Na^+ ions as blockers of H^+ currents." *Biochim. Biophys. Acta*, 987(1), 8-14.

- Hille, B. (1966). "Common mode of action of three agents that decrease the transient change in sodium permeability in nerves." *Nature*, 210(42), 1220-1222.
- Hodgkin, A. L. and Huxley, A. F. (1990). "A quantitative description of membrane current and its application to conduction and excitation in nerve. 1952." *Bull. Math. Biol.*, 52(1-2), 25-71.
- Hollmann, M. and Seifert, W. (1989). "Glutamate transport and not glutamate receptor binding is stimulated by gangliosides in a Ca²⁺-dependent manner in rat brain synaptic plasma membranes." *J. Neurochem.*, 53(3), 716-723.
- Hollmann, M., Maron, C., and Heinemann, S. (1994). "N-glycosylation site tagging suggests a three transmembrane domain topology for the glutamate receptor GluR1." *Neuron*, 13(6), 1331-1343.
- Hunter, P. R. (1998). "Cyanobacterial toxins and human health." *Soc. Appl. Bacteriol. Symp. Ser.*, 27, 35S-40S.
- Ikeda, K., Nagasawa, M., Mori, H., Araki, K., Sakimura, K., Watanabe, M., Inoue, Y., and Mishina, M. (1992). "Cloning and expression of the epsilon 4 subunit of the NMDA receptor channel." *FEBS Lett.*, 313(1), 34-38.
- Ishii, T., Moriyoshi, K., Sugihara, H., Sakurada, K., Kadotani, H., Yokoi, M., Akazawa, C., Shigemoto, R., Mizuno, N., Masu, M., and . (1993). "Molecular characterization of the family of the N-methyl-D-aspartate receptor subunits." *J. Biol. Chem.*, 268(4), 2836-2843.
- Jalonen, T., Johansson, S., Holopainen, I., Oja, S. S., and Arhem, P. (1990). "Single-channel and whole-cell currents in rat cerebellar granule cells." *Brain Res.*, 535(1), 33-38.
- Kano, M. and Kato, M. (1987). "Quisqualate receptors are specifically involved in cerebellar synaptic plasticity." *Nature*, 325(6101), 276-279.
- Keleti, G., Sykora, J. L., Lippy, E. C., and Shapiro, M. A. (1979). "Composition and biological properties of lipopolysaccharides isolated from *Schizothrix calcicola* (Ag.) Gomont (Cyanobacteria)." *Appl. Environ. Microbiol.*, 38(3), 471-477.
- Keleti, G. and Sykora, J. L. (1982). "Production and properties of cyanobacterial endotoxins." *Appl. Environ. Microbiol.*, 43(1), 104-109.
- Kimelberg, H. K., Anderson, E., and Kettenmann, H. (1990). "Swelling-induced changes in electrophysiological properties of cultured astrocytes and oligodendrocytes. II. Whole-cell currents." *Brain Res.*, 529(1-2), 262-268.
- Koch, R. A. and Barish, M. E. (1994). "Perturbation of intracellular calcium and hydrogen ion regulation in cultured mouse hippocampal neurons by reduction of the sodium ion concentration gradient." *J. Neurosci.*, 14(5 Pt 1), 2585-2593.

- Koh, J. Y. and Choi, D. W. (1987). "Quantitative determination of glutamate mediated cortical neuronal injury in cell culture by lactate dehydrogenase efflux assay." *J. Neurosci. Methods*, 20(1), 83-90.
- Leist, M., Volbracht, C., Kuhnle, S., Fava, E., Ferrando-May, E., and Nicotera, P. (1997). "Caspase-mediated apoptosis in neuronal excitotoxicity triggered by nitric oxide." *Mol. Med.*, 3(11), 750-764.
- Li, W. I., Berman, F. W., Okino, T., Yokokawa, F., Shioiri, T., Gerwick, W. H., and Murray, T. F. (2001). "Antillatoxin is a marine cyanobacterial toxin that potently activates voltage-gated sodium channels." *Proc. Natl. Acad. Sci. U. S. A.*, 98(13), 7599-7604.
- Longuemare, M. C., Rose, C. R., Farrell, K., Ransom, B. R., Waxman, S. G., and Swanson, R. A. (1999). "K(+)-induced reversal of astrocyte glutamate uptake is limited by compensatory changes in intracellular Na⁺ ." *Neuroscience*, 93(1), 285-292.
- Lucas, D. R. and Newhouse, J. P. (1957) The toxic activity of sodium-L-glutamate on the inner layers of the retina. *Arch. Ophthalmol.* 58: 193-201
- Manev, H., Favaron, M., Guidotti, A., and Costa, E. (1989). "Delayed increase of Ca²⁺ influx elicited by glutamate: role in neuronal death." *Mol. Pharmacol.*, 36(1), 106-112.
- Masu, M., Tanabe, Y., Tsuchida, K., Shigemoto, R., and Nakanishi, S. (1991). "Sequence and expression of a metabotropic glutamate receptor." *Nature*, 349(6312), 760-765.
- McGeer, E.G. and McGeer, P.L. (1976) Duplication of biochemical changes of Huntington's chorea by intrastriatal injection of glutamic and kainic acids. *Nature* 263: 517-519.
- Meldrum, B. (1985). "Possible therapeutic applications of antagonists of excitatory amino acid neurotransmitters." *Clin. Sci. (Lond)*, 68(2), 113-122.
- Mori, H., Masaki, H., Yamakura, T., and Mishina, M. (1992). "Identification by mutagenesis of a Mg(2+)-block site of the NMDA receptor channel." *Nature*, 358(6388), 673-675.
- Moriyoshi, K., Masu, M., Ishii, T., Shigemoto, R., Mizuno, N., and Nakanishi, S. (1991). "Molecular cloning and characterization of the rat NMDA receptor." *Nature*, 354(6348), 31-37.
- Narahashi, T. (1974). "Chemicals as tools in the study of excitable membranes." *Physiol Rev.*, 54(4), 813-889.
- Nicholls, D. and Attwell, D. (1990). "The release and uptake of excitatory amino acids." *Trends Pharmacol. Sci.*, 11(11), 462-468.

- Nicholls, D. G. (1989). "Release of glutamate, aspartate, and gamma-aminobutyric acid from isolated nerve terminals." *J. Neurochem.*, 52(2), 331-341.
- Nicholls, D. G. and Budd, S. L. (1998). "Neuronal excitotoxicity: the role of mitochondria." *Biofactors*, 8(3-4), 287-299.
- Noda, M., Ikeda, T., Suzuki, H., Takeshima, H., Takahashi, T., Kuno, M., and Numa, S. (1986). "Expression of functional sodium channels from cloned cDNA." *Nature*, 322(6082), 826-828.
- Nogle, L. M., Okino, T., and Gerwick, W. H. (2001). "Antillatoxin B, a neurotoxic lipopeptide from the marine cyanobacterium *Lyngbya majuscula*." *J. Nat. Prod.*, 64(7), 983-985.
- Olney, J. W. and Sharpe, L. G. (1969). "Brain lesions in an infant rhesus monkey treated with monosodium glutamate." *Science*, 166(903), 386-388.
- Olney, J. W. (1969). "Glutamate-induced retinal degeneration in neonatal mice. Electron microscopy of the acutely evolving lesion." *J. Neuropathol. Exp. Neurol.*, 28(3), 455-474.
- Olney, J. W. and de Gubareff, T. (1978). "Glutamate neurotoxicity and Huntington's chorea." *Nature*, 271(5645), 557-559.
- Olney, J. W. and de Gubareff, T. (1978). "Glutamate neurotoxicity and Huntington's chorea." *Nature*, 271(5645), 557-559.
- Orjala, J., Nagle, D., and Gerwick, W. H. (1995). "Malyngamide H, an ichthyotoxic amide possessing a new carbon skeleton from the Caribbean cyanobacterium *Lyngbya majuscula*." *J. Nat. Prod.*, 58(5), 764-768.
- Pellegrini-Giampietro, D. E., Cherici, G., Alesiani, M., Carla, V., and Moroni, F. (1988). "Excitatory amino acid release from rat hippocampal slices as a consequence of free-radical formation." *J. Neurochem.*, 51(6), 1960-1963.
- Pin, J. P. and Duvoisin, R. (1995). "The metabotropic glutamate receptors: structure and functions." *Neuropharmacology*, 34(1), 1-26.
- Rothman, S. M. (1985). "The neurotoxicity of excitatory amino acids is produced by passive chloride influx." *J. Neurosci.*, 5(6), 1483-1489.
- Schinder, A. F., Olson, E. C., Spitzer, N. C., and Montal, M. (1996). "Mitochondrial dysfunction is a primary event in glutamate neurotoxicity." *J. Neurosci.*, 16(19), 6125-6133.
- Schramm, M., Eimerl, S., and Costa, E. (1990). "Serum and depolarizing agents cause acute neurotoxicity in cultured cerebellar granule cells: role of the glutamate

- receptor responsive to N-methyl-D-aspartate." *Proc. Natl. Acad. Sci. U. S. A.*, 87(3), 1193-1197.
- Schramm, M., Eimerl, S., and Costa, E. (1990). "Serum and depolarizing agents cause acute neurotoxicity in cultured cerebellar granule cells: role of the glutamate receptor responsive to N-methyl-D-aspartate." *Proc. Natl. Acad. Sci. U. S. A.*, 87(3), 1193-1197.
- Seeburg, P. H. (1993). "The TINS/TiPS Lecture. The molecular biology of mammalian glutamate receptor channels." *Trends Neurosci.*, 16(9), 359-365.
- Siesjo, B. K., Agardh, C. D., and Bengtsson, F. (1989). "Free radicals and brain damage." *Cerebrovasc. Brain Metab Rev.*, 1(3), 165-211.
- Siman, R., Noszek, J. C., and Kegerise, C. (1989). "Calpain I activation is specifically related to excitatory amino acid induction of hippocampal damage." *J. Neurosci.*, 9(5), 1579-1590.
- Skulberg, O. M. (1972). "[Blue-green algae in Norwegian inland waters. The possible health consequences in man and animals]." *Tidsskr. Nor Laegeforen.*, 92(12), 851-853.
- Sommer, B., Keinanen, K., Verdoorn, T. A., Wisden, W., Burnashev, N., Herb, A., Kohler, M., Takagi, T., Sakmann, B., and Seeburg, P. H. (1990). "Flip and flop: a cell-specific functional switch in glutamate-operated channels of the CNS." *Science*, 249(4976), 1580-1585.
- Stout, A. K., Raphael, H. M., Kanterewicz, B. I., Klann, E., and Reynolds, I. J. (1998). "Glutamate-induced neuron death requires mitochondrial calcium uptake." *Nat. Neurosci.*, 1(5), 366-373.
- Stuhmer, W., Conti, F., Suzuki, H., Wang, X. D., Noda, M., Yahagi, N., Kubo, H., and Numa, S. (1989). "Structural parts involved in activation and inactivation of the sodium channel." *Nature*, 339(6226), 597-603.
- Suchanek, B., Seeburg, P. H., and Sprengel, R. (1995). "Gene structure of the murine N-methyl D-aspartate receptor subunit NR2C." *J. Biol. Chem.*, 270(1), 41-44.
- Sugihara, H., Moriyoshi, K., Ishii, T., Masu, M., and Nakanishi, S. (1992). "Structures and properties of seven isoforms of the NMDA receptor generated by alternative splicing." *Biochem. Biophys. Res. Commun.*, 185(3), 826-832.
- Tamkun, M. M. and Catterall, W. A. (1981). "Reconstitution of the voltage-sensitive sodium channel of rat brain from solubilized components." *J. Biol. Chem.*, 256(22), 11457-11463.
- Tanabe, Y., Masu, M., Ishii, T., Shigemoto, R., and Nakanishi, S. (1992). "A family of metabotropic glutamate receptors." *Neuron*, 8(1), 169-179.

- Tecoma, E. S., Monyer, H., Goldberg, M. P., and Choi, D. W. (1989). "Traumatic neuronal injury in vitro is attenuated by NMDA antagonists." *Neuron*, 2(6), 1541-1545.
- Wafford, K. A., Bain, C. J., Le Bourdelles, B., Whiting, P. J., and Kemp, J. A. (1993). "Preferential co-assembly of recombinant NMDA receptors composed of three different subunits." *Neuroreport*, 4(12), 1347-1349.
- Westerberg, E., Monaghan, D. T., Cotman, C. W., and Wieloch, T. (1987). "Excitatory amino acid receptors and ischemic brain damage in the rat." *Neurosci. Lett.*, 73(2), 119-124.
- White, R. J. and Reynolds, I. J. (1996). "Mitochondrial depolarization in glutamate-stimulated neurons: an early signal specific to excitotoxin exposure." *J. Neurosci.*, 16(18), 5688-5697.
- Wo, Z. G. and Oswald, R. E. (1995). "Unraveling the modular design of glutamate-gated ion channels." *Trends Neurosci.*, 18(4), 161-168.
- Wu, C. H., Huang, J. M., Vogel, S. M., Luke, V. S., Atchison, W. D., and Narahashi, T. (1985). "Actions of Ptychodiscus brevis toxins on nerve and muscle membranes." *Toxicon*, 23(3), 481-487.
- Yokokawa, F., Asano, T., and Shioiri, T. (2000). "Total synthesis of the antiviral marine natural product (-)-hennoxazole A." *Org. Lett.*, 2(26), 4169-4172.
- Yoshizawa, S., Matsushima, R., Watanabe, M. F., Harada, K., Ichihara, A., Carmichael, W. W., and Fujiki, H. (1990). "Inhibition of protein phosphatases by microcystins and nodularin associated with hepatotoxicity." *J. Cancer Res. Clin. Oncol.*, 116(6), 609-614.

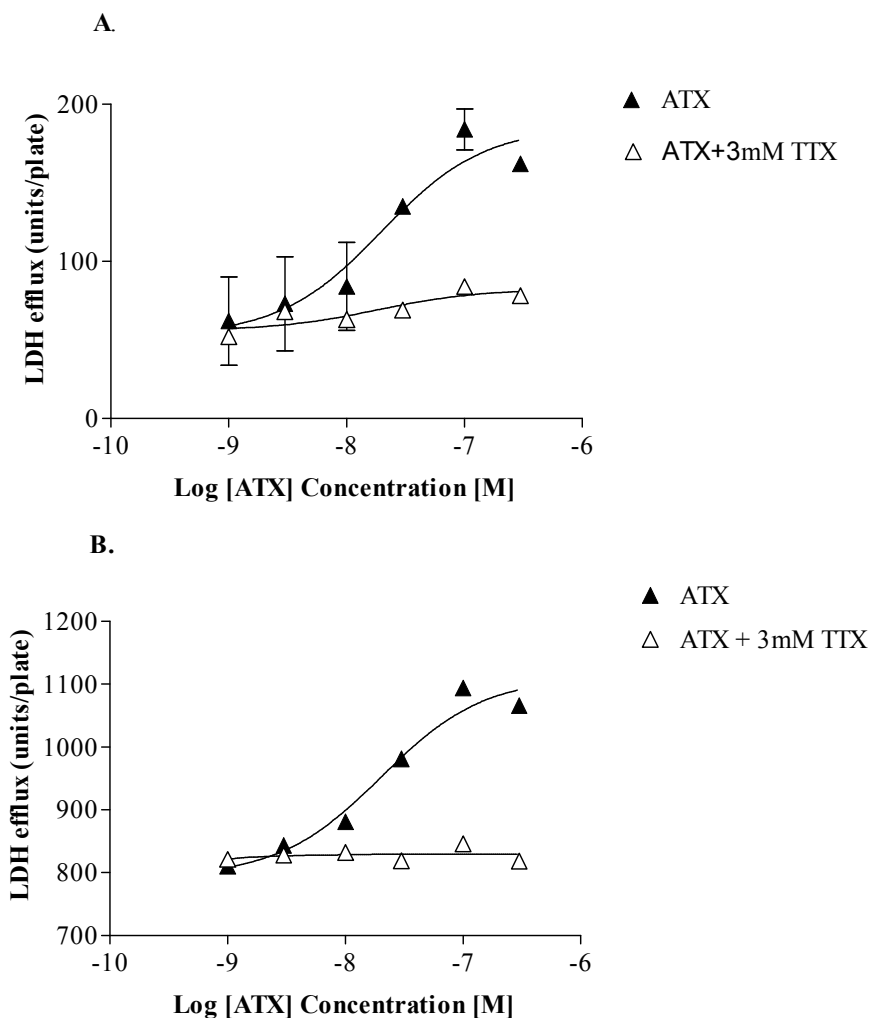


Fig. 1. Concentration-response profiles for LDH efflux from 10-12 DIC CGN exposed to varying concentrations of ATX alone (▲) and in the presence of 3 mM TTX (●). The LDH efflux after 2 h of exposure (A). The sum of the LDH activity that was released from neurons during the 2 h exposure and 22 h post exposure periods (B). Values represent LDH activity in excess of non-exposed controls that were run in parallel with treated neurons. LC50 values for 2 h and 22 h LDH accumulations were 18.22 ± 1.6 and $28.34 \pm .6$ nM, respectively. Experiments were ran in triplicates, which were repeated twice.

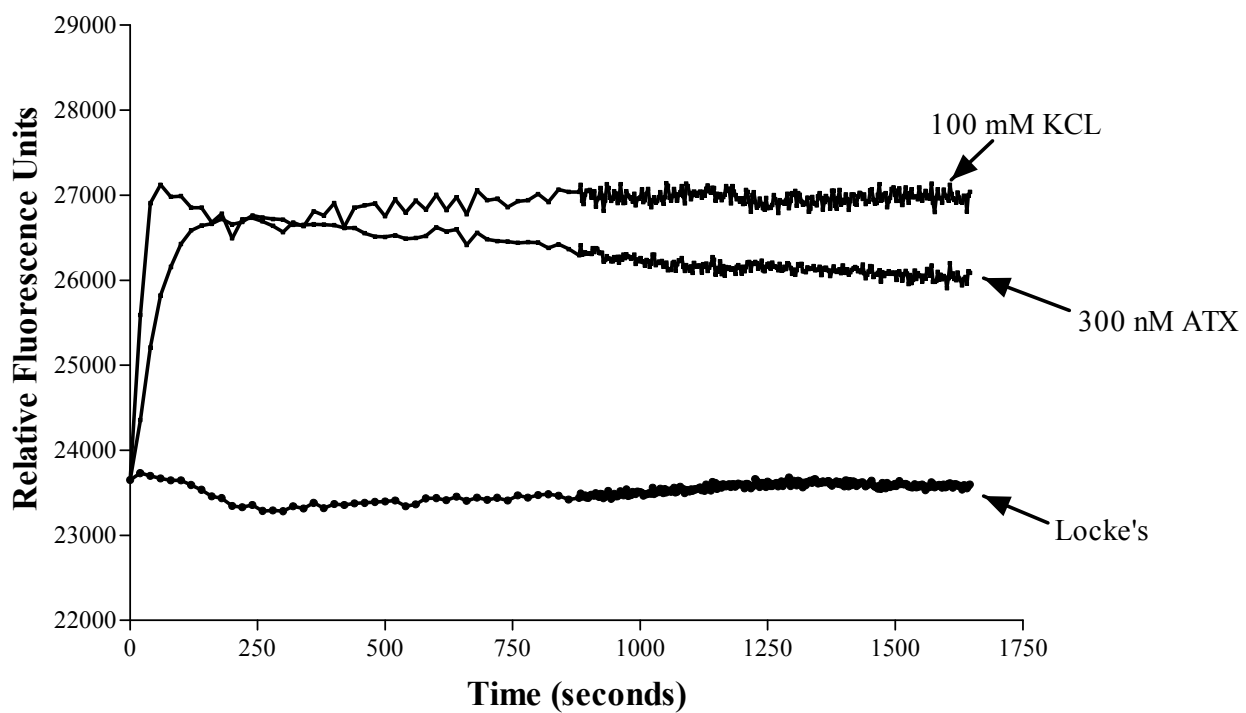


Fig. 2. Relative change in DiBAC fluorescence in CGN 10-12 DIC exposed to 100 mM KCL, 300 nM ATX and Locke's buffer.

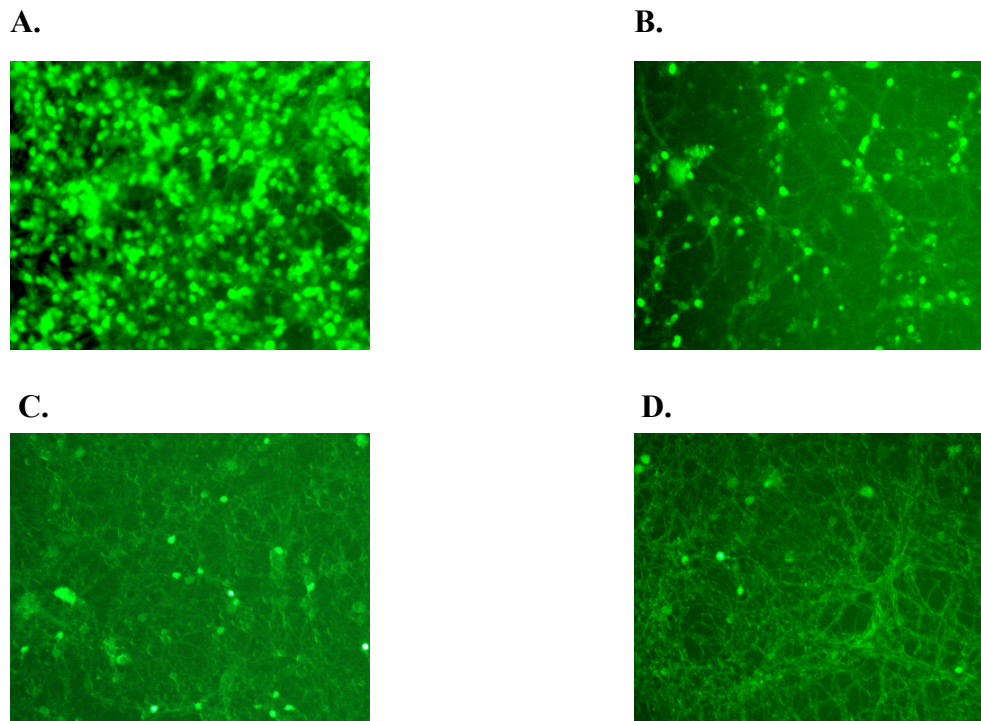


Fig. 3. Morphology of 12 DIC rat CGNs exposed to 100 nM ATX. Neurons were stained during ATX exposure with the vital dye fluorescein diacetate (5 $\mu\text{g}/\text{ml}$). **(A)** Nonexposed control neurons. **(B)** Neurons exposed 5 mins. to ATX. **(C)** Neurons exposed to ATX for 30 mins. **(D)** Neurons exposed to ATX for 2 hrs.

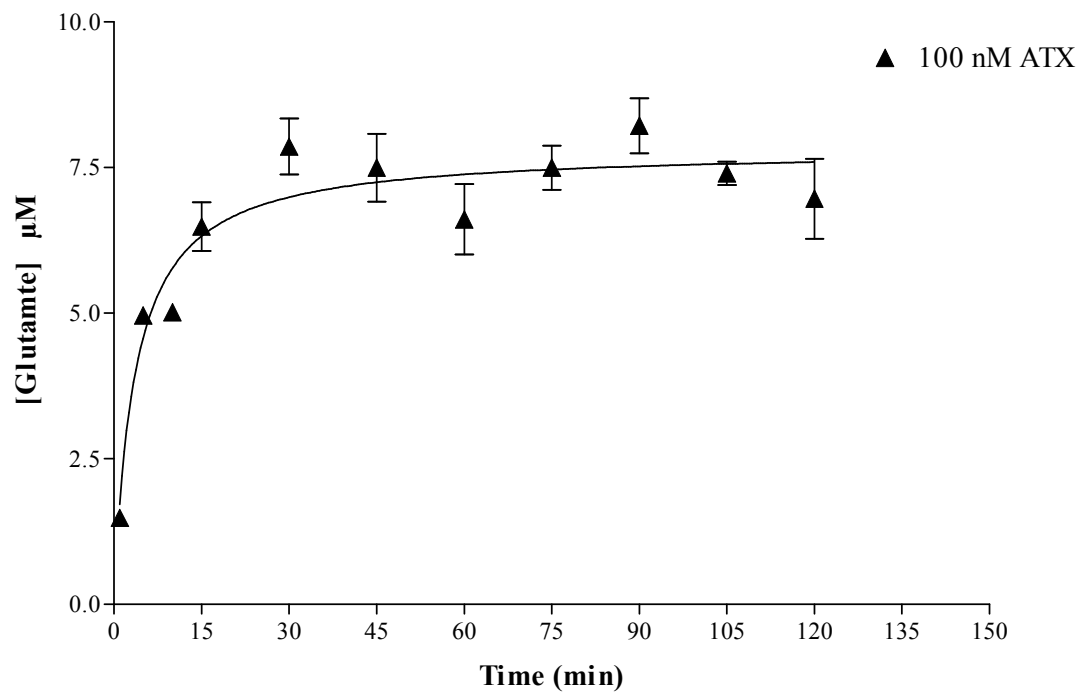


Fig. 4. Time-course of glutamate efflux from 10-12 DIC CGN exposed to 100 nM ATX. Data are from a representative experiment. Each data point represents the mean \pm S.E.M. from triplicate plates.

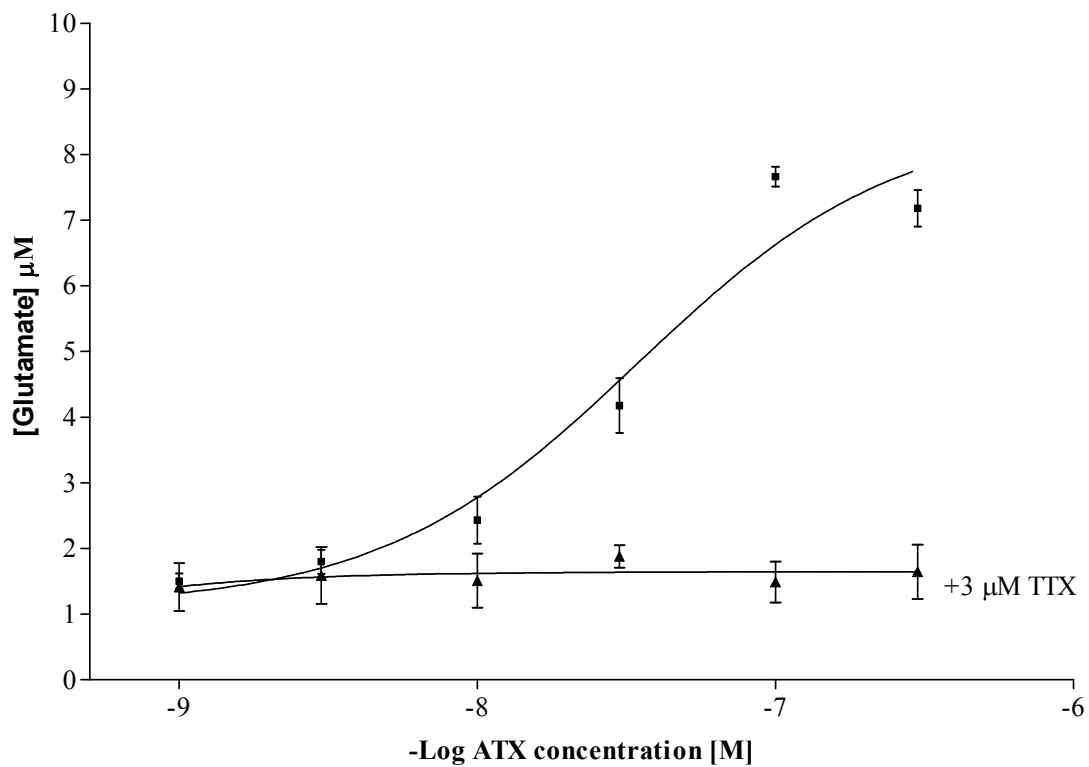


Fig. 5. Concentration-response profiles for glutamate efflux from 10-12 DIC CGN exposed for 30 min to ATX alone (■) and in the presence of 3 μM TTX (▲). Data are pooled from two experiments performed in triplicate. Each data point represents the mean ± S.E.M. from triplicate plates.

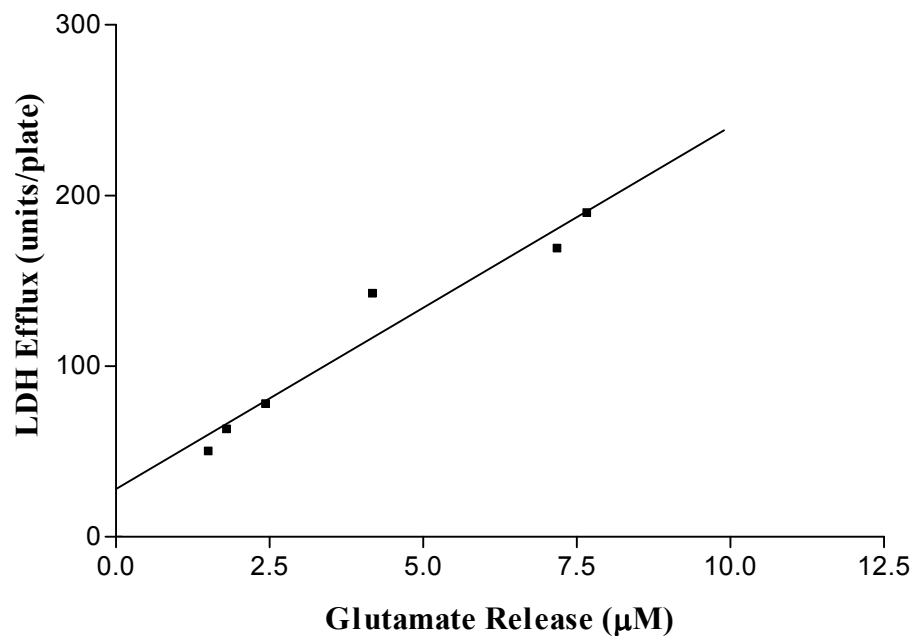
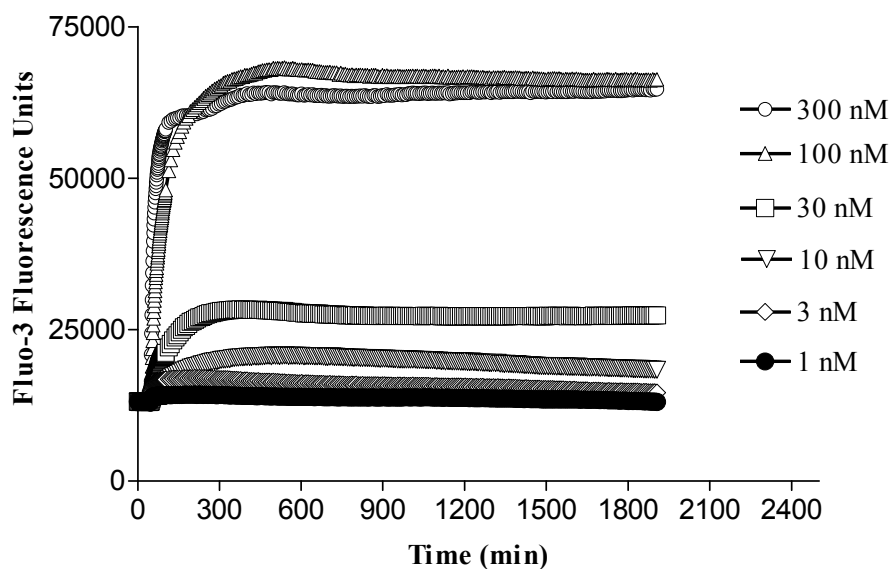


Fig. 6. Correlation between concentration-dependent glutamate release and LDH efflux. Glutamate release was measured after a 30 min exposure to ATX while LDH efflux was determined after 2 h incubation. The displayed regression line was determined from a linear regression analysis ($r^2 = .9482$, $p < .001$). LDH data are taken from fig. 1A. Glutamate release values are derived from fig. 5.

A.



B.

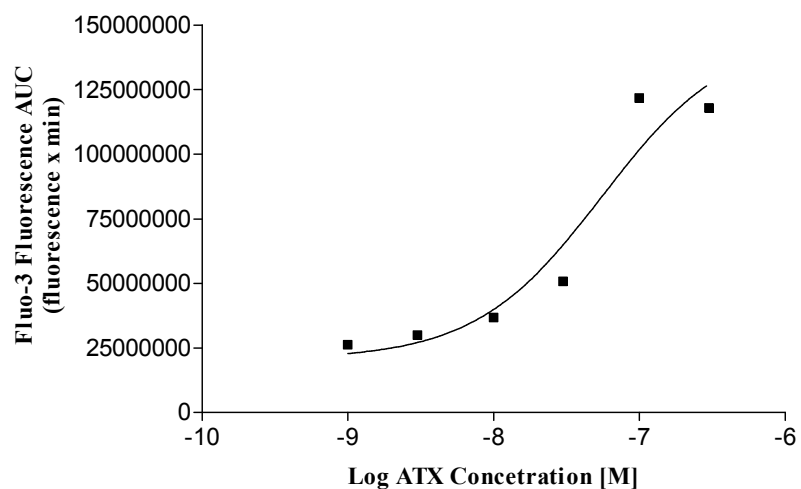


Fig. 7. (A) Increases in fluo-3 fluorescence produced by exposing 10-13 DIC CGN to varying concentrations of ATX. Basal fluo-3 fluorescence, which was approximately 10,000-15,000 U in each experiment, was automatically subtracted from each data point by the FLIPR software. (B) Non-linear regression analysis of the integrated fluo-3 fluorescence response [area under the curve (AUC)] versus ATX concentration data ($EC_{50} = 55.6$ nM).

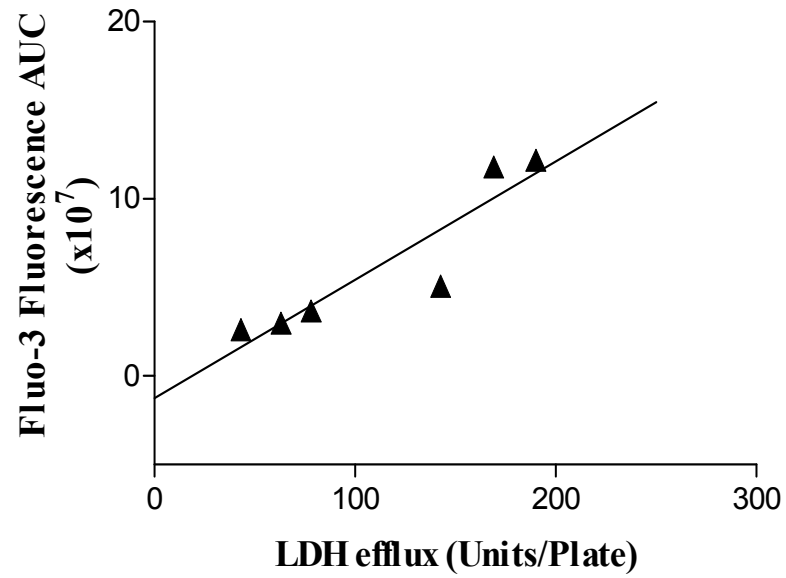


Fig. 8. Correlation between fluo-3 AUC and LDH efflux. The displayed regression line was determined from a linear regression analysis ($r^2 = .8475$, $p < .001$). LDH data are taken from fig. 1A. Fluo-3 AUC values are derived from fig. 7B.

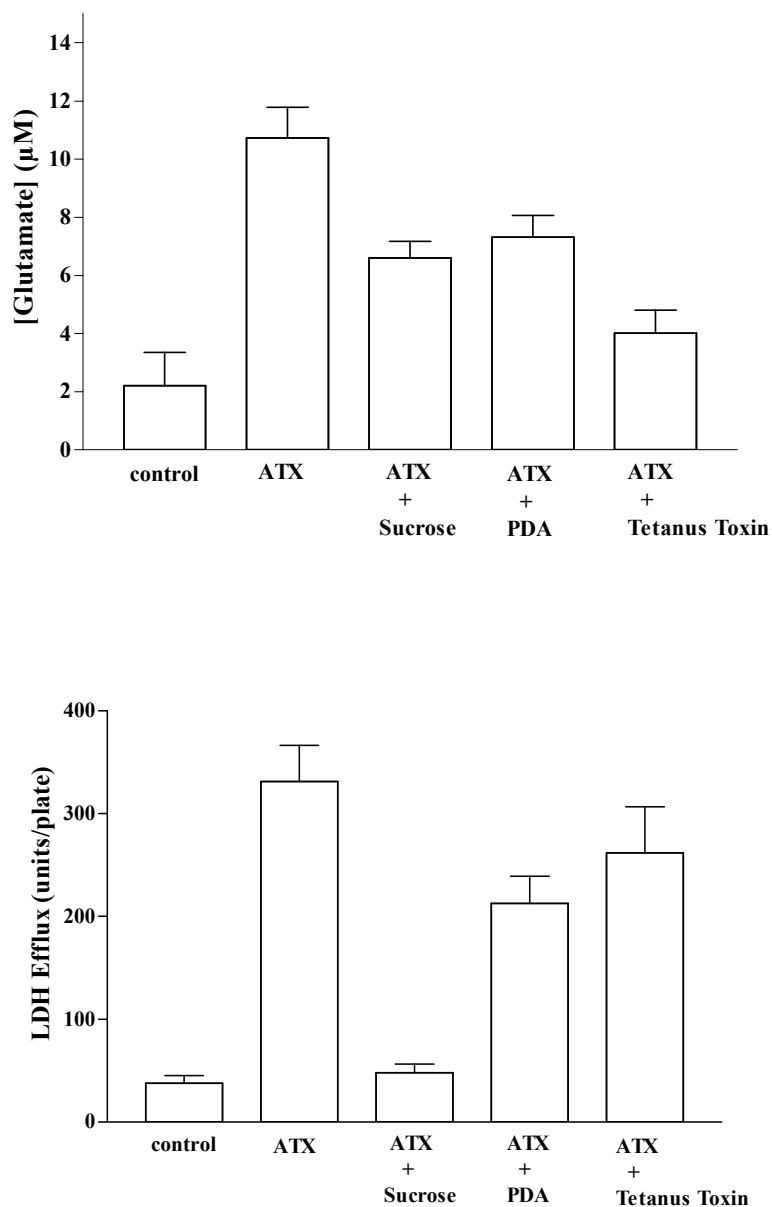


Fig. 9. Effect of treatment with glutamate release antagonists 100 mM sucrose, 200 μM PDA, and 37.5 nM tetanus toxin on glutamate release (A) and LDH efflux (B) exposed to 100 nM ATX for 30 mins (A) and 24 hrs (B). Values represent means \pm S.E.M. from at least 3 experiments.